Hindawi
Journal of Mathematics
Volume 2024, Article ID 6652037, 30 pages
https://doi.org/10.1155/2024/6652037

*Research Article*

# Modeling and Analysis of an Age-Structured Malaria Model in the Sense of Atangana–Baleanu Fractional Operators

**Dawit Kechine Menbiko and Chernet Tuge Deressa**

*College of Natural Sciences, Department of Mathematics, Jimma University, Jimma, Ethiopia*

Correspondence should be addressed to Dawit Kechine Menbiko; abgiadawit@gmail.com

Received 29 August 2023; Revised 21 November 2023; Accepted 13 December 2023; Published 8 January 2024

Academic Editor: Mubashir Qayyum



In this paper, integer- and fractional-order models are discussed to investigate the dynamics of malaria in a human host with a varied age distribution. A system of differential equation model with five human state variables and two mosquito state variables was examined. Preschool-age (0–5) and young-age individuals make up our model's division of the human population. We investigated the existence of an area in which the model is both mathematically and epidemiologically well posed. According to the findings of our mathematical research, the disease-free equilibrium exists whenever the fundamental reproduction number $R_0$ is smaller than one and is asymptotically stable. The disease-free equilibrium point is unstable when $R_0 > 1$. We showed that the endemic equilibrium point is unique for $R_0 > 1$. Also, the most influential control parameters of the spread of malaria were identified. Numerical simulations of both classical and fractional order were conducted, and we used ODE (45) for classical part and numerical technique developed by Toufik and Atangana for fractional order. The infected population will grow because of the high biting frequency of the mosquito and the high likelihood of transmission from the infected mosquito to the susceptible human. $R = 1.622$, which is more than one, indicating that the mosquito vector keeps on growing. This supports the stability of the endemic equilibrium point theorem, which states that the disease becomes endemic when $R = 1$. The susceptible human population will decrease because of the presence of the infective mosquito, which has a high biting frequency for the first couple of days. Since the infective mosquito bit the susceptible human, the susceptible human became infected and went to the infected human compartments. Then, the susceptible population will decrease and the infested human population will increase. After a certain amount of time, it becomes zero due to the growth of protected classes. In this case, a disease-free equilibrium point exists and is stable. This condition exists because $R_0 = 2.827 \times 10^{-5}$ is less than 1. This supports the theorem that the stability of the disease-free equilibrium point is obtained when $R_0 < 1$. Depending on equation, we have shown that the possibility of some endemic equilibria exists when $R_0 < 1$, that is, it undergoes backward bifurcation, even when the disease-free equilibrium is locally stable, and the result means that the society may misunderstand the level of malaria prevalence in the community.

## 1. Introduction

Vector-borne diseases (VBDs) result from an infection communicated by vectors such as mosquitoes, ticks, lice, and fleas. These vectors carry pathogenic organisms such as bacteria, viruses, fungi, protists, and parasitic worms which can be transferred from one host to another. Some examples of VBDs are dengue fever, Lyme disease, malaria, West Nile virus, Rift Valley fever, and Japanese encephalitis [1]. In many tropical and subtropical regions, malaria is a prevalent and potentially fatal infectious disease. It is brought on by the *Plasmodium* parasite, which is spread when female *Anopheles* mosquitoes bite people to obtain blood for their eggs [2]. The most prevalent species of *Plasmodium* are *Plasmodium vivax* in temperate zones and *Plasmodium falciparum* in tropical areas [3, 4]. About half of the world's population is in danger of malaria, according to the WHO (World Health Organization) malaria report [5]. Globally, there were estimated 228 million cases of malaria and 405000 deaths from it in 2018. Most of these cases and deaths accounted for 93% and 94% of all malaria cases globally in 2018. The projected number of cases and fatalities from malaria in 2019 was 229 million worldwide [6]. Globally, there were reportedly 247 million cases of malaria in 2021, with 619000 deaths attributed to the disease.

A disproportionately large amount of the worldwide malaria burden is placed on the WHO African Region. 95% of malaria cases and 96% of malaria deaths in 2021 occurred in the area. Almost 80% of all malaria deaths in the WHO African Area occurred in children under the age of five. Two-thirds of recorded deaths are children [6]. As they have not yet acquired immunity to illnesses, children under the age of five are more susceptible to malaria than adults [7]. As a result, the age distribution in a community affects the spread of malaria. In Ethiopia, 60% and 40% of malaria cases are caused by the species *Plasmodium falciparum* and *Plasmodium vivax*, respectively [8, 9]. Many scientific attempts have been made, including the creation of mathematical models, to lessen the impact of malaria on the global community. Ross, in 1911 [10], applied deterministic compartmental epidemic models to illustrate the dynamics of malaria infection between vector and host populations. Macdonald and Ross's model [11] was modified by adding biological data about mosquito latency brought on by the growth of the malaria parasite. Nonetheless, efforts to stop the spread of malaria have resulted in the creation of effective vector control measures, including larvicide, indoor residual spraying, and insecticide-treated nets (ITNs) [6, 12]. Non-integer-order calculus has more than 300-year history. Many theories are being added to the literature on fractional calculus every day. In the seventeenth century, German mathematician Gottfried Leibniz and well-known British scientist Isaac Newton developed the idea of fractional calculus as a result of calculus's ramifications. In the form of generalized fractional order, fractional calculus deals with the definitions of classical calculus [13]. In order to comprehend, forecast, and manage the spread of diseases among populations, mathematical modeling of infectious diseases is essential. Through the integration of mathematical tools and epidemiological knowledge, researchers are able to conduct scenario simulations, investigate diverse intervention options, and facilitate the making of public health decisions. These models are useful instruments for educating decision-makers and supporting the creation of winning plans to fight infectious illnesses and safeguard the public's health [14].

A novel mathematical model was recently presented by Mohammed-Awel and Gumel [15], because of the widespread use of indoor residual spraying (IRS) and insecticide-treated nets (ITNs) for malaria control, for evaluating the impact of pesticide resistance in the mosquito population. In [1, 16], fractional-order derivatives are described as nonlinear systems in a more realistic way in comparison with integer-order derivatives, and a comparison of temperature distribution via Atangana–Baleanu non-integer-order fractional derivatives is used to illustrate the application of the mathematical technique of Laplace transform. Many fractional derivatives have been developed by researchers and used in a variety of scientific and engineering fields [17–19], and the most frequently used derivatives in the various branches of science, particularly in mathematical epidemiology, are Caputo, Caputo–Fabrizio (CF), and Atangana–Baleanu (AB). Different kernel properties apply to each of these three fractional derivatives. In contrast to Caputo–Fabrizio, which uses an exponentially decaying type kernel (which is nonsingular but nonlocal), AB derivative in the Caputo sense uses a Mittag-Leffler type kernel. Odibat just developed a brand-new fractional derivative of the generalized Caputo type [20]. The features of this novel generalized Caputo derivative are comparable to those of Caputo derivatives [21]. A nonlinear fractional-order model for analyzing the dynamical behavior of vector-borne diseases within the frame of Caputo-fractional derivative was analyzed, numerical simulations for different values of fractional-order derivative were performed, and a comparison with the results of the integer-order derivative was made. In this study, the nature of our malaria model is read at non-integer-order values using Atangana–Baleanu fractional derivatives with a high efficiency rate.

The advantage of using CF and AB fractional derivatives to solve the projected malaria disease model is that they provide strong approaches for the arbitrary order case, memory effects, and crossover behavior of the model.

The benefit of using the Atangana–Baleanu operator is that it incorporates the crossover behavior of the malaria disease dynamics model as well as memory results. It also has a nonsingular and non-nearby kernel, which enables us to explain complex structures that uniquely, incredibly, and efficiently observe both the law of electricity and exponential decay at the same time. Here, we consider the integer-order model proposed by "Klinck" in [15] and modify it to become fractional-order models in the Atangana–Baleanu–Caputo sense. After recalling some definitions and results concerning integer-order and fractional-order derivatives, we prove the existence and give conditions under the fractional models that admit a unique solution. To illustrate our analytical results, we shall adopt the Toufik–Atangana method to perform numerical simulations for the fractional model. Researchers in [15] worked on the dynamics of malaria in an age-structured human host; in their model, human population was partitioned into two compartments: preschool age $(0-5)$ and the rest of the human population. They have divided the human population into two classes: $H_1$ and $H_2$, having $S, I$, and $R$ compartments in each class. Thus, the human population $N_H$ is divided into six compartments, and we modify such integer-order model proposed in [15] by including the parameter of natural recovery rate of both age groups in addition to the recovery rate due to treatment and the protected group of human population to measure the effect of intervention mechanisms such as insecticide-treated nets (ITNs) and indoor residual spraying (IRS) in the transmission dynamics of malaria and fractional-order models in the Atangana–Baleanu–Caputo sense to describe the memory effects and crossover behavior of the malaria model. For simplicity, we consider only one susceptible and recovery compartment, respectively, for both age groups of human population. The aim of our study is to understand the dynamics of malaria through integer-order and fractional-order analysis of age-structured malaria model.

This study is organized as follows. In Section 2, we develop mathematical model formulation. Section 3 gives the model analysis. Section 4 presents the numerical simulation of the integer-order malaria model. Section 5 gives the fractional malaria model and analysis. Section 6 presents the numerical scheme and simulation of the fractional-order model. Section 7 gives the result and discussion. Section 8 draws the conclusion.

## 2. Formulation of Modified Mathematical Model

The human population, denoted by $N_h$, is divided into five epidemiological categories: the susceptible class $S_h$, the protected class $P_h$, the infectious class of preschool age $I_c$, the infectious class of young age $I_y$, and the recovered class $R_h$. We also divide the mosquito population into two major stages: the mature stage and the aquatic stage (egg, larvae, and pupae), but we consider the mature stage which is divided into two compartments, namely, susceptible class of mosquitoes denoted by $S_m$ and infectious class of mosquitoes denoted by $I_m$. The mosquitoes' population does not have a recovered class because their infective period ends with their death. At any time $t$, the total size of the human $N_h(t)$ and mature mosquitoes $N_m(t)$ is, respectively, denoted by

$$\begin{aligned} N_h(t) &= S_h(t) + P_h(t) + I_C(t) + I_y(t) + R_h(t),\\ N_m(t) &= S_m(t) + I_m(t). \end{aligned} \tag{1}$$

Through birth, people are added to society at a constant rate ($\Lambda_h$). Of those added, those protected by specific protective measures belong to the protected class $P_h$, while the remaining ($(1-\gamma)\Lambda_h$) belong to the susceptible class ($S_h$). The susceptible people who heard recommendations and implement protective measures will join the protected class $P_h$ at the rate of $\tau$. In our model, individuals belonging to the susceptible class are at risk of infection at a rate of ($\lambda_c$) for the infectious class $I_c$ (pre-school age) and at a rate of $\lambda_y$ for the infectious class $I_y$ (young - age). The infected individuals of both age levels recover spontaneously at the natural recovery rate of $\omega_1$ and $\omega_2$ and treatment recovery rate of $\delta_1$ and $\delta_2$, respectively, to join the recovery class $R_h$. Some studies [22, 23] indicated that the recovered humans have some immunity to the disease and do not get clinically ill, but they still harbor low levels of the parasite in their bloodstream and can pass the infection to mosquitoes. After a certain amount of time, they lose their immunity at a rate $\beta$ and the proportion $\beta\phi$ returns to the susceptible class and the remaining $(1-\phi)\beta R$ who take some protective measurements enter into the protected class. Since the malaria interventions might face serious obstacles in the form of heterogeneity in parasite, vector, and human population [24], the protected humans may become susceptible again and move to the susceptible class $S_h$ at the rate $\phi$. Humans leave the total population through natural death rate $\mu_h$ and malaria death rate (disease-induced death rate) $\mu_d$. When a susceptible mosquito $S_m$ bites an infectious human, it enters into class $I_c$ and $I_y$ with fraction of bite $K_2$. Mosquitoes are assumed to suffer death due to natural causes and due to the use of insecticide spray at a rate $\mu_m$ or mortality due to insecticides but cannot die directly from the malaria parasite infection [25]; female mosquitoes enter their population through the susceptible compartment at per capita rate $\Lambda_m$. It is assumed that there is no immigration of infectious individuals in the human population. The death related to the disease is different between children (preschool aged) and young-aged people, i.e., $\mu_{d_1}$ is greater than $\mu_{d_2}$ [26]. We also assume that infectious preschool-age children mature and join the corresponding infectious young-age class at the rate of $\eta$.

In Figure 1, red lines show disease progression and solid and black lines show human or mosquito progression from one compartment to another compartment. Based on the above assumptions and flow diagram, the dynamics of the disease were described by the following nonautonomous deterministic system of nonlinear DEs.

$$\begin{cases} \dfrac{dS_h}{dt} = (1-\gamma)\Lambda_h + \varphi P_h + \beta\Phi R_h - \left(\tau + \lambda_c + \lambda_y + \mu_h\right)S_h,\\[2ex] \dfrac{dP_h}{dt} = \gamma\Lambda_h + \tau S_h + (1-\Phi)\beta R_h - (\varphi + \mu_h)P_h,\\[2ex] \dfrac{dI_C}{dt} = \lambda_C S_h - \left(\mu_{d_1} + \mu_h + \eta + (\omega_1 + \delta_1)\right)I_C,\\[2ex] \dfrac{dI_y}{dt} = \lambda_y S_h + \eta I_C - \left(\mu_{d_2} + \mu_h + (\omega_2 + \delta_2)\right)I_y,\\[2ex] \dfrac{dR_h}{dt} = \left((\omega_2 + \delta)I_y + (\omega_1 + \delta_1)\right)I_C - (\beta\phi + (1-\phi)\beta + \mu_h)R_h,\\[2ex] \dfrac{dS_m}{dt} = \Lambda_m - (\lambda_m + \mu_m)S_m,\\[2ex] \dfrac{dI_m}{dt} = \lambda_m S_m - \mu_m I_m, \end{cases} \tag{2}$$

where

$$\begin{aligned} \lambda_m &= \frac{k_2\varepsilon_{m\left(I_C+I_y\right)S_m}}{N_h},\\ \lambda_C &= \frac{k_1\varepsilon_C I_m S_h}{N_h},\\ \lambda_y &= \frac{k_1\varepsilon_y I_m S_h}{N_h} \end{aligned} \tag{3}$$

represent the force of infection of preschool age, young age, and mosquito.

All parameters in Table 1 are positive.

## 3. Model Analysis

*3.1. Positivity of the Solution of the Model.* For the system of differential equations in (6), to ensure that the solutions of the system with positive initial conditions remain positive

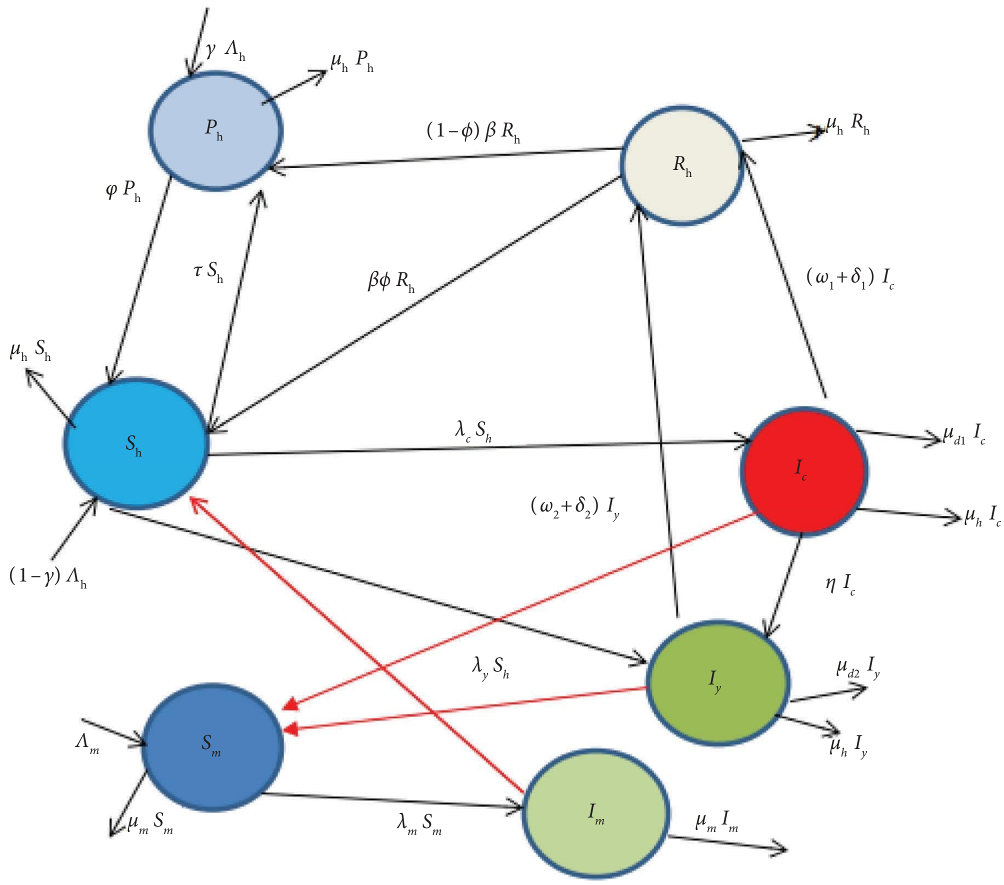


Figure 1: Flow diagram.

Table 1: Description of parameters.

| Parameter | Parameter description |
|---|---|
| $\omega_1$ | Natural recovery rate of preschool age |
| $\delta_1$ | Recovery rate by treatment of preschool age |
| $\omega_2$ | Natural recovery rate of young age |
| $\delta_2$ | Recovery rate by treatment of young age |
| $\varphi$ | Transfer rate of human from $P_h$ to $S_h$ |
| $\tau$ | Transfer rate of human from $S_h$ to $P_h$ |
| $\Lambda_h$ | Constant recruitment rate for humans |
| $\beta$ | Rate of loss of immunity |
| $\phi$ | Proportion of humans who lose their immunity that become $S_h$ |
| $(1-\phi)$ | Proportion of humans who lose their immunity that become $P_h$ |
| $\gamma$ | Proportion of new recruitments that are protected |
| $\lambda_C$ | Force of infection for preschool age |
| $\lambda_y$ | Force of infection of young age |
| $\lambda_m$ | Force of infection of mosquitoes |
| $\eta$ | Maturation rate from $I_C$ to $I_y$ |
| $\mu_{d_1}$ | Disease-induced mortality rate of preschool age |
| $\mu_{d_2}$ | Disease-induced mortality rate of young age |
| $\mu_m$ | Mortality rate of mosquitoes |
| $\mu_h$ | Natural mortality rate of human |
| $\varepsilon_c$ | Number of bites on preschool-age people |
| $\varepsilon_y$ | Number of bites on young-age people |
| $K_1$ | Fraction of bites that successfully infect human |
| $K_2$ | Fraction of bites that successfully infect mosquitoes |

for all $t > 0$, it is necessary to prove that all the state variables are nonnegative, so we have the following theorem.

**Theorem 1.** *Let $M$ be a positive region in $R_+^7$:*

$$M = \{S_h, P_h, I_c, I_y, R_h, S_m, I_m\} \in R_+^7, \tag{4}$$

*and the initial value for the malaria model (2) be*

$$\begin{aligned} &S_h(0) > 0, P_h(0) > 0, S_m(0) > 0, I_c(0) \geq 0,\\ &I_y(0) \geq 0, R_h(0) \geq 0, I_m(0) \geq 0. \end{aligned} \tag{5}$$

Then, the solution of $S_h(t), P_h(t), I_c(t), I_y(t), R_h(t), S_m(t)$, and $I_m(t)$ of the nonlinear system of differential equation above is positive for all $t > 0$.

Then, we have to prove that $S_h(0) > 0, P_h(0) > 0, I_c(0) > 0$, $I_y(0) > 0$, $S_m(0) > 0, I_m(0) > 0$; from the continuity of $S_h(t), P_h(t), I_c(t), I_y(t), R_h(t), S_m(t)$, and $I_m(t)$, we deduce that $t > 0$, $S_h(0) > 0, P_h(0) > 0, I_c(0) > 0$, $I_y(0) > 0$, $S_m(0) > 0, I_m(0) > 0$, for all $t > 0$; consider the first equation of system (2):

$$\begin{aligned} &\frac{dS}{dt} = \{(1-\gamma)\Lambda_h + \varphi P_h + \beta\phi R_h - (\tau + \lambda_c + \lambda_y + \mu_h)S_h\},\\ &\frac{dS}{dt} + (\tau + \lambda_c + \lambda_y + \mu_h)S_h = (1-\gamma)\Lambda_h + \varphi P_h + \beta\phi R_h,\\ &S_h(t) = e^{\tau+\mu_h - \int \lambda_h(t)dt} S_h(0) + e^{\tau+\mu_h - \int \lambda_h(t)dt} \int e^{\tau+\mu_h - \int \lambda_h(t)dt} (1-\gamma)\Lambda_h + \varphi P_h + \beta\phi R_h dt, \end{aligned} \tag{6}$$

since $e^{\tau+\mu_h - \int \lambda_h(t)dt} > 0, S_h(0) > 0$, and $P_h(t) > 0, R_h(t) > 0$; also, exponential function is always positive; then, the solution $S_h(t) > 0$.

Similarly, all state variables at $t$ could not be zero and positive. From this, we conclude that all the solutions of (2) are in $R_+^7$ for all $t > 0$ provided that initial conditions are positive.

*3.2. Invariant Region.* The invariant region is a region where solutions of model equation (2) exist biologically [27]. Biological entities cannot be negative; therefore, all the solutions of model equation (2) are positive for all time $t \geq 0$ [27]. The total population size $N_h$ and $N_m$ can be defined as in equation (1). In the absence of malaria disease, the DEs for $N_h$ are given as

$$\frac{dN_h}{dt} \leq \Lambda - \mu_h N_h \Longrightarrow N_h(0) \leq \frac{\Lambda_h}{\mu_h}. \tag{7}$$

The DEs for $N_m$ are also given as

$$N_m(0) \leq \frac{\Lambda_m}{\mu_m}. \tag{8}$$

**Theorem 2.** *Model (2) has a feasible solution which is contained in the region*

$$M = \{S_h, P_h, I_c, I_y, R_h, S_m, I_m\} \in R_+^7. \tag{9}$$

*Proof.* Let

$$\{S_h, P_h, I_c, I_y, R_h, S_m, I_m\} \in R_+^7 \tag{10}$$

be any solution of the system with nonnegative initial condition. Using (7),

$$\begin{aligned} &\frac{dN_h}{dt} \leq \Lambda_h - \mu N_h \Lambda \int d(N_h e^{\mu_h}) \leq \Lambda_h \int e^{\mu_h t} dt,\\ &N_h \leq \frac{\Lambda_h}{\mu_h} + \left(N_{h_0} - \frac{N_h}{\mu_h}\right)e^{-\mu_h t}. \end{aligned} \tag{11}$$

Therefore, as $t \longrightarrow 0$, the human population $N_h$ approaches $\Lambda_h/\mu_h$, and it follows that [24]

$$\begin{aligned} &\lim_{t\longrightarrow\infty} \sup N_h(t) \leq \frac{\Lambda_h}{\mu_h},\\ &\lim_{t\longrightarrow\infty} \sup N_m(t) \leq \frac{\Lambda_m}{\mu_m}. \end{aligned} \tag{12}$$

Therefore, the feasible solution set for model (2) is given by

$$\begin{aligned} &M = \{S_h, P_h, I_c, I_y, R_h, S_m, I_m\} \in R_+^7,\\ &(S_h, P_h, S_m) > 0, N_h \leq \frac{\Lambda_h}{\mu_h}, N_m \leq \frac{\Lambda_m}{\mu_m}. \end{aligned} \tag{13}$$

Hence, the compact set $M$ is positively invariant, and the solutions are bounded (i.e., all solutions with initial conditions in $M$ remain in $M$ for all time $t$). □

*3.3. Disease-Free Equilibrium Point.* At the disease-free equilibrium, all the disease classes are zero. It is a scenario which depicts an infection-free state in the community or society. Further, at the disease equilibrium point of people and mosquitoes, $I_c = 0, I_y = 0, I_m = 0$. Disease-free equilibrium of system is given by $\varepsilon_0 = (S_h^0, P_h^0, 0, 0, 0, S_m^0, 0)$, where

$$\begin{aligned}
P_h^0 &= \frac{(\tau + \gamma\eta_h)\Lambda_h}{\left(\tau + \mu_{h+\varphi}\right)\mu_h},\\
S_h^0 &= \frac{(\varphi + (1-\gamma)\mu_h)\Lambda_h}{(\tau + \mu_h + \varphi)\mu_h},\\
N_h(0) &= P_h^0 + S_h^0 = \frac{\Lambda_h}{\mu_h},\\
N_m(0) &= \frac{\Lambda_m}{\mu_m}.
\end{aligned} \tag{14}$$

*3.3.1. The Basic Reproduction Number.* The average number of secondary cases a typical infected person produces in their entire life as infectious or an infectious period when introduced or allowed to exist in a group of susceptible individuals is known as the basic reproduction number or $R_0$ [28]. $R_0$ is a threshold quantity computed using the next-generation method which is used to handle the future dynamical behavior of the pandemic and used to study the spread of an infectious disease in epidemiological modeling [28, 29]. It is defined as

$$R_0 = \rho\left(FV^{-1}\right) \quad \text{where} \quad FV^{-1} = \left(\frac{\partial F}{\partial x}(\varepsilon_0)\right)\left(\frac{\partial v}{\partial x}(\varepsilon_0)\right)^{-1}, \tag{15}$$

using the next-generation method.

The dominant eigenvalue or reproduction number becomes

$$R_0 = \sqrt{\left(\frac{K_2\varepsilon_m S_m^0}{bN_h^0}\right)\left(\frac{K_1\varepsilon_y S_h^0}{\mu_m N_h^0}\right) + \left(\frac{K_2\varepsilon_m S_m^0}{aN_h^0} + \frac{\eta K_2\varepsilon_m S_m^0}{abN_h^0}\right)\left(\frac{K_1\varepsilon_c S_h^0}{\mu_m N_h^0}\right)}, \tag{16}$$

for

$$\begin{aligned}
a &= \mu_{d_1} + \mu_h + \omega_1 + \delta_1,\\
b &= \mu_{d_2} + \mu_h + \omega_2 + \delta_2,
\end{aligned} \tag{17}$$

which is the average number of secondary infections caused by a single infective in a totally susceptible population.

*3.4. Local Stability of Disease-Free Equilibrium Point*

**Theorem 3.** *The disease-free equilibrium point of the system of ordinary differential equation (2) is locally asymptotically stable if $R_0 < 1$ and unstable if $R_0 > 1$.*

*Proof.* To show the local stability of disease-free equilibrium point, we use $(7 \times 7)$ Jacobian matrix and the Routh–Hurwitz (RH) criterion.

$$J(\varepsilon_0) = \begin{pmatrix}
c & \varphi & 0 & 0 & \beta\Phi & 0 & -V_1\\
\tau & M_1 & 0 & 0 & (1-\Phi)\beta & 0 & 0\\
0 & 0 & a & 0 & 0 & 0 & V_2\\
0 & 0 & \eta & b & 0 & 0 & V_3\\
0 & 0 & (\omega_1 + \delta_1) & (\omega_2 + \delta_2) & f & 0 & 0\\
0 & 0 & -V_4 & -V_5 & 0 & g & 0\\
0 & 0 & V_4 & V_5 & 0 & 0 & M_2
\end{pmatrix}, \tag{18}$$

and let $c = -(\tau - \mu_h), M_1 = -(\varphi + \mu_h), a = -(\mu_{d_1} + \mu_h + \eta + \omega + \delta_1), b = -(\mu_{d_2} + \delta_2 + \omega_2 + \delta_2), f = -(\beta + \mu_h), g = -\mu_m$, $M_2 = -\mu_m$.

$$J(\varepsilon_0) = \begin{pmatrix} c-\lambda & \varphi & 0 & 0 & \beta\Phi & 0 & -V_1 \\ \tau & M_1-\lambda & 0 & 0 & (1-\Phi)\beta & 0 & 0 \\ 0 & 0 & a-\lambda & 0 & 0 & 0 & V_2 \\ 0 & 0 & \eta & b-\lambda & 0 & 0 & V_3 \\ 0 & 0 & (\omega_1+\delta_1) & (\omega_2+\delta_2) & f-\lambda & 0 & 0 \\ 0 & 0 & -V_4 & -V_5 & 0 & g-\lambda & 0 \\ 0 & 0 & V_4 & V_5 & 0 & 0 & M_2-\lambda \end{pmatrix},$$
$$V_1 = \left(\frac{K_1\varepsilon_c S_h^0}{N_h^0} + \frac{K_1\varepsilon_y S_h^0}{N_h^0}\right),$$
$$V_2 = \frac{K_1\varepsilon_c S_h^0}{N_h^0},$$
$$V_3 = \frac{K_1\varepsilon_y S_h^0}{N_h^0},$$
$$V_4 = \frac{K_2\varepsilon_m S_m^0}{N_h^0},$$
$$-V_5 = \frac{K_2\varepsilon_m S_m^0}{N_h^0}. \tag{19}$$

We consider only the first and the second column of $7 \times 7$ matrix; when we consider the fifth and the seventh column, we will get zero matrix because of zero column matrix. Through the reduction process, we obtain two negative eigenvalues $\lambda_1 = -\mu_m$ and $\lambda_2 = -(\beta + \mu_h)$ and the reduced submatrix becomes

$$[(C-\lambda)(M_1-\lambda) - \varphi(\tau)]\begin{pmatrix} a-\lambda & 0 & V_2 \\ \eta & b-\lambda & V_3 \\ V_4 & V_5 & \mu_m - \lambda. \end{pmatrix}, \tag{20}$$

and the characteristic equation of the first submatrix,

$$(C-\lambda)(M_1-\lambda) - \varphi(\tau) = 0, \tag{21}$$

is

$$A_2\lambda^2 - A_1 + A_0 = 0, \tag{22}$$

where $A_2 = 1, A_1 = (C + M_1), A_0 = CM_1 - \varphi\tau$, and all coefficients $A_i$ of submatrix (21) of the characteristic equation and the first column of the RH array are positive, so by the RH stability criterion, the two eigenvalues $\lambda_3$ and $\lambda_4$ of Jacobian have negative real part. The second submatrix is given by

$$\begin{pmatrix} a-\lambda & 0 & V_2 \\ \eta & b-\lambda & V_3 \\ V_4 & V_5 & \mu_m - \lambda. \end{pmatrix} = 0, \tag{23}$$

and the characteristic equation of the second submatrix is

$$A_3\lambda^3 - A_2\lambda^2 + A_1\lambda + A_0 = 0, \tag{24}$$

where

$$\begin{aligned} &A_3 = -1, A_2 = (a + b + M_2), \\ &A_1 = (V_2V_4 + V_3V_5 - aM_2 - bM_2 - ab), \\ &A_0 = abM_2 + V_2V_5\eta - aV_3V_5 - V_2V_4b. \end{aligned} \tag{25}$$

All the first columns of the RH array are positive; then, the remaining eigenvalues of the Jacobian are negative real part for $R_0 < 1$. Thus, the disease-free equilibrium point $\varepsilon_0$ is locally asymptotically stable for $R_0 < 1$ and unstable for $R_0 > 1$. □

*3.5. Global Stability of Disease-Free Equilibrium Point*

**Theorem 4.** *If the reproduction number $R_0 < 1$, the disease-free equilibrium point $\varepsilon_0$ of model (2) is globally asymptotically stable in the feasible region $M$.*

*Proof.* To prove the global asymptotic stability of the disease-free equilibrium point $\varepsilon_0$, we use the method of Lyapunov function. Let us define an appropriate Lyapunov function $V(t)$ by applying the approach in [27]. $V = C_1I_c + C_2I_y + C_3I_m$, where $C_1, C_2, C_3$ are positive constants and $I_c, I_y$, and $I_m$ are positive state variables.

$$\frac{dv}{dt} = C_1\frac{dI_c}{dt} + C_2\frac{dI_y}{dt} + C_3\frac{dI_m}{dt}. \tag{26}$$

By substituting expressions for $dI_c/dt, dI_y/dt$, and $dI_m/dt$ from (2) in (26) and by collecting like terms of the equation, we obtain

$$\begin{aligned}\frac{\mathrm{d}v}{\mathrm{d}t} &= C_1\frac{k_1\varepsilon_c I_m S_h}{N_h} - C_1 a I_c + c_2\frac{k_1\varepsilon_y I_m S_h}{N_h} + C_2\eta I_c - C_2 b I_y \\ &\quad + C_3\frac{k_2\varepsilon_m I_c S_m}{N_h} + C_3\frac{k_2\varepsilon_m I_y S_m}{N_h} - C_3\mu_m I_m + C_3\frac{k_2\varepsilon_m I_m S_m}{N_h} + C_2\eta - C_1 a = 0,\end{aligned} \tag{27}$$

and by taking coefficients of $I_c$ and $I_y$ equal to zero for $dv/dt \leq 0$,

$$C_3\frac{k_2\varepsilon_m I_m S_m}{N_h} - C_2 b = 0, \tag{28}$$

$$\begin{aligned}\frac{\mathrm{d}v}{\mathrm{d}t} &= C_1\frac{k_1\varepsilon_c I_m S_h}{N_h} \\ &\quad + C_1\frac{k_2\varepsilon_y I_y S_h}{N_h} - C_3\mu_m I_m,\end{aligned} \tag{29}$$

$$C_3\frac{K_2\varepsilon_m S_m}{N_h} + C_2\eta - C_1 a = 0. \tag{30}$$

From (28),

$$C_2 = C_3\frac{k_2\varepsilon_m I_m S_m}{bN_h}. \tag{31}$$

By substituting $C_2$ in (30), we obtain

$$C_1 = C_3\left(\frac{k_2\varepsilon_m S_m}{aN_h} + \frac{k_2\varepsilon_m S_m}{\eta}abN_h\right). \tag{32}$$

After substituting $C_1$ and $C_2$ in (29) and after some calculation, we obtain $[R_0^2 - 1]I_m \leq 0$; from this, for $I_m = 0$, $R_0 \leq 1$. Finally, we obtain $\mathrm{d}v/\mathrm{d}t \leq 0$; then, $\mathrm{d}v/\mathrm{d}t = 0$. This shows that the disease-free equilibrium is globally asymptotically stable. □

*3.6. Endemic Equilibrium Point.* Endemic equilibrium points are steady-state solutions where the disease persists in the population. The solution for the endemic equilibrium is obtained in terms of the infected humans, which is also expressed in terms of $R_0$.

**Theorem 5.** *If $R_0 > 1$, then the system of DEs of the model has a unique endemic equilibrium point.*

$$\varepsilon^* = \left(S_h^*, P_h^*, I_c^*, I_y^*, R_h^*, S_m^*, I_m^*\right). \tag{33}$$

*Proof.* After some algebraic manipulation, we have

$$\begin{aligned}S_h^* &= \frac{P_1\pi}{\pi P_4 + \left(P_2K_1\varepsilon_c + P_3K_1\varepsilon_y\right)I_m^*}, \\ I_c^* &= \frac{P_1\pi K_1\varepsilon_c I_m^*}{\pi P_4 + a\left(P_2K_1\varepsilon_c + P_3K_1\varepsilon_y\right)I_m^*}, \\ I_y^* &= \frac{\left(K_1\varepsilon_y a + \eta K_1\varepsilon_c\right)P_1 I_m^*}{R_0^2 ab\left(P_2K_1\varepsilon_c + P_3K_1\varepsilon_y\right)I_m^* + \pi P_4}, \\ R_h^* &= \frac{P_1\left(daK_1\varepsilon_y + K_1\varepsilon_c(\eta d + be)\right)R_0^2 I_m^*}{abf\left(P_2K_1\varepsilon_c + P_3K_1\varepsilon_y\right)I_m^* + \pi P_4}, \\ P_h^* &= \frac{\left[P_1\left(\pi P_5 + K_1\varepsilon_y P_6 + P_7K_1\varepsilon_c\right) + \gamma\Lambda_h abf\left(P_2K_1\varepsilon_c + P_3K_1\varepsilon_y\right)\right]R_0^2 I_m^* + \pi P_4}{abfg_2\left(P_2K_1\varepsilon_c + P_3K_1\varepsilon_y\right)I_m^* + \pi P_4}, \\ S_m^* &= \frac{\Lambda abT_1 I_m^* + \pi P_4}{(T_2\mu_m + ab\mu_m T_1)I_m^* + \pi P_4\mu_m} \\ &\quad \cdot R_0^2\left(ab\pi\mu_m T_1\left(T_2\mu_m + ab\mu_m T_1\right)\right)I_m^{*^3} \\ &\quad + \left(ab\pi^2\mu_m^2 T_1 P_4 + R_0^2\left(\pi P_4\left(T_2\mu_m + ab\mu_m T_1\right) - T_3P_1\Lambda abT_1\right)\right)I_m^{*^2} \\ &\quad + \left(\pi P_4(1 + \mu_m) - T_3P_1\pi P_4\right)I_m^*,\end{aligned} \tag{34}$$

and after some steps and simplification, the degree three polynomial is reduced to quadratic:

$$AI_m^{*^2} + BI_m^* + C = 0, \tag{35}$$

and at $I^* = 0$, there was DFE.

$$\begin{aligned} A &= R_0^2\left(ab\pi\mu_m T_1\left(T_2\mu_m + ab\mu_m T_1\right)\right),\\ B &= \left(ab\pi^2\mu_m^2 T_1 p_4 + R_0^2\left(\pi p_4\left(T_2\mu_m + ab\mu_m T_1\right) - T_3 p_1 \Lambda ab T_1\right)\right),\\ C &= \frac{\mu_h^2}{p_1\Lambda^2\mu_m^2(ab)^2}\left(\frac{\mu_m + 1}{\mu_m}\left(1 - R_0^2\right)\right), \end{aligned} \tag{36}$$

where $P_1 = \Lambda g_2 \text{abf}\mu_h, P_2 = g_2\text{abf} + (d\eta + be), P_3 = g_2\text{abf} - (\beta(\varphi + \phi\mu_h))da, P_4 = g_2 abf\mu_h, T_1 = p_2k_1\varepsilon_c + p_3k_1, T_2 = p_1(k_2\varepsilon_m k_1\varepsilon_c + ak_2\varepsilon_m(k_1\varepsilon_y a + \eta k_1\varepsilon_c)), T_3 = bk_2\varepsilon_m k_1\varepsilon_c + k_2\varepsilon_m(k_1\varepsilon_y a + \eta k_1\varepsilon_c)$ contains parameters.

From quadratic equation (35), the endemic equilibrium exists for

$$B^2 - 4AC \geq 0. \tag{37}$$

The number of possible positive real roots for (35) depends on the signs of A, B, and C. This can be analyzed by using the Descartes rule of signs on the quadratic

$$f\left(I_m^*\right) = AI_m^{*^2} + BI_m^* + C. \tag{38}$$

As indicated in [30], Descartes's rule of sign is used to determine the number of real zeros of a polynomial function; it indicates that the number of positive real zeros in a polynomial function $f(I_m^*)$ is equal to or less than the number of coefficient sign changes, on an even number basis.

In Table 2, the existence of multiple endemic equilibria when $R_0 < 1$ suggests the possibility of backward bifurcation. The change of stability occurring at $R_0 = 1$ is often followed by the emergence of branch of steady states. This is referred to as bifurcation; this may happen for values of $R_0$ slightly greater than one which is called forward bifurcation, and if $R_0$ is slightly less than one, this is called backward bifurcation. In quadratic equation (15),

$$\begin{aligned} I_m^* &= \frac{-B + \sqrt{B^2 - 4AC}}{2A},\\ I_m^* &= \frac{-B - \sqrt{B^2 - 4AC}}{2A}. \end{aligned} \tag{39}$$

If $R_0 > 1$ or $C < 0$, then (15) has a unique positive root:

$$I_m^* = \frac{-B + \sqrt{\Delta}}{2A}, \tag{40}$$

where $\Delta > 0$. If $R_0 = 0$ or $C = 0$, then (15) has a unique positive solution. $I_m^* = -B/2A$, provided that $B < 0$. Here, if $B = 0$, then $I_m^* = 0$ which shows DFE $\varepsilon_0$, and if $B > 0$, then $I_m^* < 0$, and this does not show meaning in epidemiology. For $R_0 < 1$ or $C > 0$ and $\Delta > 0$, we consider two cases.

(i) If $B > 0$, then $I_m^* < 0$, that is, (15) has no solution.
(ii) If $B < 0$, that is, if $B < -2\sqrt{AC} < 0$, then (15) has two endemic equilibria.

By considering such different cases of the solution of (15), a theorem is established as follows. □

**Theorem 6.** *The age-structured malaria model has*

*(1) A unique endemic equilibrium if*

*(a) $C < 0$ iff $R_0 > 0$*
*(b) $B < 0$ and $C = 0$ or $B^2 - 4AC = 0$*

*(2) Two endemic equilibria if $C > 0, B < 0,$ and $B^2 - 4AC > 0$.*

*(3) No endemic equilibrium in all other ways.*

In the theorem for $R_0 < 1$, stable DFE and stable EE come together; this indicates the probability of backward bifurcation. Analysis of backward bifurcation was carried out by employing center manifold theory.

*3.6.1. Center Manifold Theory.* Computation of eigenvalues of the Jacobian matrix can be used to determine the stability of the disease at an endemic equilibrium point. The bifurcation analysis is performed at the disease-free equilibrium by using center manifold theory as presented in Martcheva [28]. To apply the center manifold theory, the following simplification and change of variables are made on the model which are rewritten by using state variables of malaria model and center manifold approach on the system.

Let $X_1 = S_h,, X_2 = P_h, X_3 = I_c, X_4 = I_y, X_5 = R_h, X_6 = S_m, X_7 = I_m$,

$$\begin{aligned} N_h &= X_1 + X_2 + X_3 + X_4 + X_5,\\ N_m &= X_6 + X_7. \end{aligned} \tag{41}$$

Further by using the vector,

$$X = \left(X_1, X_2, X_3, X_4, X_5, X_6, X_7\right)^T. \tag{42}$$

The system can be written in the form

$$F = \left(f_1, f_2, f_3, f_4, f_5, f_6, f_7\right)^T \tag{43}$$

Table 2: Number of possible real roots of $f(I_m^*)$ for $R_0 > 1$ and $R_0 < 1$.

| Cases | $A$ | $B$ | $C$ | $R_0$ | Number of sign changes | Number of +ve real roots |
|---|---|---|---|---|---|---|
| 1 | + | + | + | <1 | 0 | 1 |
| 2 | + | − | + | <1 | 2 | 1 |
| 3 | − | + | + | <1 | 1 | 2 |
| 4 | − | − | + | <1 | 1 | 0 |
| 5 | + | + | − | >1 | 1 | 2 |
| 6 | + | − | − | >1 | 1 | 1 |
| 7 | − | + | − | >1 | 2 | 1 |
| 8 | − | − | − | >1 | 0 | 0 |

and as follows writing the system in vector forms:

$$\frac{\mathrm{d}x}{\mathrm{d}t} = F(x_i), \tag{44}$$

$$\begin{cases} \dfrac{\mathrm{d}X_1}{\mathrm{d}t} = f_1 = (1-\gamma)\Lambda_h + \varphi X_2 + \beta\Phi X_5 - \left(\tau X_1 - \dfrac{k_1\varepsilon_c X_7 X_1}{N_h} - \dfrac{k_1\varepsilon_y X_7 X_1}{N_h} - \mu_h X_1\right), \\ \dfrac{\mathrm{d}X_2}{\mathrm{d}t} = f_2 = \gamma\Lambda_h + \tau X_1 + (1-\Phi)\beta X_5 - (\varphi + \mu_h)X_2, \\ \dfrac{\mathrm{d}X_3}{\mathrm{d}t} = f_3 = \dfrac{k_1\varepsilon_c X_7 X_1}{N_h} - \left(\mu_{d_1} + \mu_h + \eta + (\omega_1 + \delta_1)\right)X_3, \\ \dfrac{\mathrm{d}X_4}{\mathrm{d}t} = f_4 = \dfrac{k_1\varepsilon_y X_7 X_1}{N_h} + \eta X_3 - \left(\mu_{d_2} + \mu_h + (\omega_2 + \delta_2)\right)X_4, \\ \dfrac{\mathrm{d}X_5}{\mathrm{d}t} = f_5 = ((\omega_2 + \delta)X_4 + (\omega_1 + \delta_1))X_3 - (\beta\phi + (1-\phi)\beta + \mu_h)X_5, \\ \dfrac{\mathrm{d}X_6}{\mathrm{d}t} = f_6 = \Lambda_m - \dfrac{k_2\varepsilon_m (X_3 + X_4)X_6}{N_h} + \mu_h X_6, \\ \dfrac{\mathrm{d}X_7}{\mathrm{d}t} = f_7 = \dfrac{k_2\varepsilon_m (X_3 + X_4)X_6}{N_h} - \mu_m X_7. \end{cases} \tag{45}$$

Choose $k_1$ as bifurcation parameter, and solving for $R_0 = 1$,

$$k_1 = \frac{abN_h^2\mu_m}{ak_2\varepsilon_m S_m \varepsilon_y S_h + (bk_2\varepsilon_m S_m \mu_m + \eta k_2 \varepsilon_m \mu_m S_m)\varepsilon_c abS_h}. \tag{46}$$

The Jacobian matrix evaluated at disease-free equilibrium:

$$J(\varepsilon_0) = \begin{pmatrix} c & \varphi & 0 & 0 & \beta\Phi & 0 & -V_1, \\ \tau & M_1 & 0 & 0 & (1-\Phi)\beta & 0 & 0 \\ 0 & 0 & a & 0 & 0 & 0 & V_2 \\ 0 & 0 & \eta & b & 0 & 0 & V_3 \\ 0 & 0 & (\omega_1 + \delta_1) & (\omega_2 + \delta_2) & f & 0 & 0 \\ 0 & 0 & -V_4 & -V_5 & 0 & g & 0 \\ 0 & 0 & V_4 & V_5 & 0 & 0 & M_2 \end{pmatrix}. \tag{47}$$

Eigenvalues of Jacobian are $\lambda_1 = -\mu_m, \lambda_2 = -(\beta + \mu_h)$,

$$\lambda_3 = \frac{-(C+m_1)+\sqrt{(C+m_1)^2-4(Cm_1-\varphi)}}{2},$$
$$\lambda_4 = \frac{-(C+m_1)-\sqrt{(C+m_1)^2-4(Cm_1-\varphi)}}{2}. \quad (48)$$

Using RH criteria, the remaining eigenvalues of Jacobian are negative real for $R_0 < 1$. Hence, the center manifold theory can be used to analyze the dynamics of the system for the case when $R_0 - 1$, and it can be shown that the Jacobian matrix has a right eigenvector.

$$W = \begin{pmatrix} W_1 \\ W_2 \\ W_3 \\ W_4 \\ W_5 \\ W_6 \\ W_7 \end{pmatrix} \cdot \begin{pmatrix} c & \varphi & 0 & 0 & \beta\Phi & 0 & -V_1 \\ \tau & M_1 & 0 & 0 & (1-\Phi)\beta & 0 & 0 \\ 0 & 0 & a & 0 & 0 & 0 & V_2 \\ 0 & 0 & \eta & b & 0 & 0 & V_3 \\ 0 & 0 & (\omega_1+\delta_1) & (\omega_2+\delta_2) & f & 0 & 0 \\ 0 & 0 & -V_4 & -V_5 & 0 & g & 0 \\ 0 & 0 & V_4 & V_5 & 0 & 0 & M_2 \end{pmatrix} \begin{pmatrix} W_1 \\ W_2 \\ W_3 \\ W_4 \\ W_5 \\ W_6 \\ W_7 \end{pmatrix},$$
$$W_1 = \frac{k_1}{\mathrm{abf}\tau}\left[\frac{M_2C(1-\phi)+\tau\phi-(1-\phi)(\tau\phi-CM_2)}{(\tau\varphi-CM_2)}+V_1\tau\right]W_7,$$
$$W_2 = \left[\frac{[\beta(\omega_1+\delta_1)V_2b+(\omega_2+\delta_2)(\eta V_2+aV_3)]}{\mathrm{abf}(\tau\varphi-CM_2)}(C(1-\phi)+\tau\phi)+V_1\tau\right]W_7,$$
$$W_3 = \frac{V_2W_7}{a},$$
$$W_4 = \left(\frac{\eta V_2+aV_3}{ab}\right)W_7,$$
$$W_5 = \frac{[(\omega_1+\delta_1)V_2b+(\omega_2+\delta_2)(\eta V_2+aV_3)]W_7}{\mathrm{abf}},$$
$$W_6 = \frac{-(V_4V_2b+V_5(\eta V_2+aV_3))W_7}{\mathrm{abg}}. \quad (49)$$

Similarly, the components of the left eigenvector of $J$ correspond to zero eigenvalue, and it can be done by transposing Jacobian matrix.

$$\begin{pmatrix} c & \varphi & 0 & 0 & \beta\Phi & 0 & -V_1 \\ \tau & M_1 & 0 & 0 & (1-\Phi)\beta & 0 & 0 \\ 0 & 0 & a & 0 & 0 & 0 & V_2 \\ 0 & 0 & \eta & b & 0 & 0 & V_3 \\ 0 & 0 & (\omega_1+\delta_1) & (\omega_2+\delta_2) & f & 0 & 0 \\ 0 & 0 & -V_4 & -V_5 & 0 & g & 0 \\ 0 & 0 & V_4 & V_5 & 0 & 0 & M_2 \end{pmatrix}\begin{pmatrix} y_1 \\ y_2 \\ y_3 \\ y_4 \\ y_5 \\ y_6 \\ y_7 \end{pmatrix}, \tag{50}$$

where

$$\begin{aligned} y_3 &= \left(\frac{yV_5 - V_4 b}{b}\right) y_7, \\ y_4 &= \frac{-V_5 y_7}{b}, y_7 > 0, \\ y_1 &= y_2 = y_5 = y_6 = y_7 = 0. \end{aligned} \tag{51}$$

Now, we shall establish the conditions on parameter values that cause a backward bifurcation to occur in system (45) based on the use of center manifold theory in Martcheva [28].

Computation of $a$ and $b$ for the transformed system of (45) is associated with nonzero partial derivatives of $f$ evaluated at the DFE $(S_h^0, P_h^0, 0, 0, 0, S_m^0, 0)$.

$$\begin{aligned} a &= \sum_{i,j,k=1}^{7} y_3 W_i W_j \frac{\partial^2 f_3(\varepsilon_0, k_1)}{\partial X_i \partial X_j} + \sum_{i,j,k=1}^{7} y_4 W_i W_j \frac{\partial^2 f_4(\varepsilon_0, k_1)}{\partial X_i \partial X_j} + \sum_{i,j,k=1}^{7} y_7 W_i W_j \frac{\partial^2 f_7(\varepsilon_0, k_1)}{\partial X_i \partial X_j}, \\ \frac{\partial^2 f_3}{\partial X_2 \partial X_7} &= \frac{\partial^2 f_3}{\partial X_3 \partial X_7} = \frac{\partial^2 f_3}{\partial X_5 \partial X_7} = \frac{-k_1 \varepsilon_c(\varphi + (1-\gamma)\mu_h)\mu_h}{(\tau + \mu_h + \varphi)\Lambda_h}, \\ \frac{\partial^2 f_4}{\partial X_2 \partial X_7} &= \frac{\partial^2 f_4}{\partial X_3 \partial X_7} = \frac{\partial^2 f_4}{\partial X_5 \partial X_7} = \frac{\partial^2 f_4}{\partial X_4 \partial X_7} = \frac{-k_1 \varepsilon_y(\varphi + (1-\gamma)\mu_h)\mu_h}{(\tau + \mu_h + \varphi)\Lambda_h}, \\ \frac{\partial^2 f_7}{\partial X_4 \partial X_5} &= \frac{\partial^2 f_7}{\partial X_1 \partial X_3} = \frac{\partial^2 f_7}{\partial X_1 \partial X_4} = \frac{\partial^2 f_7}{\partial X_2 \partial X_3} = \frac{\partial^2 f_7}{\partial X_2 \partial X_4} = \frac{\partial^2 f_7}{\partial X_3 \partial X_5} = \frac{-k_2 \varepsilon_m \Lambda_m \mu_h^2}{\Lambda_h^2 \mu_m}, \\ \frac{\partial^2 f_7}{\partial X_3 \partial X_4} &= \frac{\partial^2 f_7}{\partial X_4 \partial X_3} = \frac{\partial^2 f_7}{\partial X_3^2} = \frac{\partial^2 f_7}{\partial X_4^2} = \frac{-2k_2 \varepsilon_m \Lambda_m \mu_h^2}{\Lambda_h^2 \mu_m}, \\ \frac{\partial^2 f_7}{\partial X_3 \partial X_6} &= \frac{\partial^2 f_7}{\partial X_4 \partial X_6} = \frac{k_2 \varepsilon_{m\mu_h}}{\Lambda_h}\left(1 - \frac{\Lambda_m \mu_h}{\Lambda_h \mu_m}\right). \end{aligned} \tag{52}$$

It is not necessary to calculate the derivatives of $f_1, f_2, f_5, f_6$ in computing $b$ because $y_1, y_2, y_5, y_6$ are all 0. From

$$\begin{aligned} b &= \sum_{i,k=1}^{7} y_k W_i \frac{\partial^2 f_k(\varepsilon_0, k_1)}{\partial X_i \partial k_1}, \\ b &= \sum_{i,k=1}^{7} \left[ y_3 W_7 \frac{\partial^2 f_3(\varepsilon_0, k_1)}{\partial X_7 \partial k_1} + y_4 W_7 \frac{\partial^2 f_4(\varepsilon_0, k_1)}{\partial X_7 \partial k_1} \right], \\ \frac{\partial^2 f_3(\varepsilon_0, k_1)}{\partial X_7 \partial k_1} &= \frac{\varepsilon_c(\varphi + (1-\gamma)\mu_h)}{(\tau + \mu_h + \varphi)}, \\ \frac{\partial^2 f_4(\varepsilon_0, k_1)}{\partial X_7 \partial k_1} &= \frac{\varepsilon_y(\varphi + (1-\gamma)\mu_h)}{(\tau + \mu_h + \varphi)}, \\ b &= \left( y_3 W_7 \frac{\varepsilon_c(\varphi + (1-\gamma)\mu_h)}{(\tau + \mu_h + \varphi)} + y_4 W_4 \frac{\varepsilon_y(\varphi + (1-\gamma)\mu_h)}{(\tau + \mu_h + \varphi)} \right) > 0, \end{aligned} \tag{53}$$

when we come to $a$,

$$
\begin{aligned}
a &= y_3 W_7 k_1 \frac{\varepsilon_c(\varphi + (1-\gamma)\mu_h)\mu_h}{(\tau + \mu_h + \varphi)\Lambda_h}(-W_2 - W_3 - W_4 - W_5) \\
&+ y_4 W_7 k_1 \frac{\varepsilon_y(\varphi + (1-\gamma)\mu_h)\mu_h}{(\tau + \mu_h + \varphi)\Lambda_h}(-W_2 - W_3 - W_4 - W_5) \\
&+ \left[ y_7 W_3 k_2 \frac{\varepsilon_m \Lambda_m \mu_h^2}{\mu_m \Lambda_h^2} + y_7 W_4 k_2 \frac{\varepsilon_m \Lambda_m \mu_h^2}{\mu_m \Lambda_h^2} \right](-W_2 - W_1 - W_5 - 2W_3 - 2W_4) \\
&+ \left[ y_7 W_3 k_2 \frac{\varepsilon_m \mu_h}{\Lambda_h} + y_7 W_4 k_2 \frac{\varepsilon_m \mu_h}{\Lambda_h} \right]\left(1 - \frac{\Lambda_m \mu_h}{\Lambda_h \mu_m}\right) W_6 + .
\end{aligned}
\tag{54}
$$

Let

$$
\begin{aligned}
Z_1 &= -(W_2 + W_3 + W_4 + W_5), \\
Z_2 &= -(W_2 + W_1 + W_5 + 2W_3 + 2W_4), \\
a &= y_7(W_3 + W_4) k_2 \frac{\varepsilon_m \mu_h}{\Lambda_h}\left(1 - \frac{\Lambda_m \mu_h}{\Lambda_h \mu_m}\right) W_6 \\
&- \left[\left( y_3 W_7 k_1 \frac{\varepsilon_c(\varphi + (1-\gamma)\mu_h)\mu_h}{(\tau + \mu_h + \varphi)\Lambda_h} + y_4 W_7 k_1 \frac{\varepsilon_y(\varphi + (1-\gamma)\mu_h)\mu_h}{(\tau + \mu_h + \varphi)\Lambda_h}\right) Z_1 + Z_2 y_7 W_4 k_2 \frac{\varepsilon_m \Lambda_m \mu_h^2}{\mu_m \Lambda_h^2}\right].
\end{aligned}
\tag{55}
$$

Let

$$
\begin{aligned}
F_1 &= y_7(W_3 + W_4) k_2 \frac{\varepsilon_m \mu_h}{\Lambda_h}\left(1 - \frac{\Lambda \mu_h}{\Lambda_h \mu_m}\right) W_6, \\
F_2 &= -\left[\left( y_3 W_7 k_1 \frac{\varepsilon_c(\varphi + (1-\gamma)\mu_h)\mu_h}{(\tau + \mu_h + \varphi)\Lambda_h} + y_4 W_7 k_1 \frac{\varepsilon_y(\varphi + (1-\gamma)\mu_h)\mu_h}{(\tau + \mu_h + \varphi)\Lambda_h}\right) Z_1 + Z_2 y_7 W_4 k_2 \frac{\varepsilon_m \Lambda_m \mu_h^2}{\mu_m \Lambda_h^2}\right],
\end{aligned}
\tag{56}
$$

and by considering $F_1$ and $F_2$, $a$ is positive if $F_1 > F_2$. As we observed $b$ is positive, according to center manifold theory, if $a > 0, b > 0$, then the given age-structured malaria model undergoes backward bifurcation at $R_0 = 1$ whenever $b > 0$ and $F_1 > F_2$.

As we observed, an age-structured malaria model exhibits backward bifurcation whenever $a > 0$, and the epidemiological significance of backward bifurcation is that, in addition to generating $R_0 < 1$, more action is necessary to reduce the dynamics of malaria transmission in communities. Figure 2 shows the backward bifurcation phenomenon as evidence for the malaria model analysis. The stable equilibrium is represented by the solid line and the unstable equilibrium is represented by the dotted line. It confirms the results of the analysis, showing an endemic equilibrium.

*3.7. The Local Stability of the Endemic Equilibrium Point.* We conduct linear stability on the endemic equilibrium point using the Jacobian of the malaria model of the equations. Then, the following stability theorem is stated.

**Theorem 7.** *The endemic equilibrium point* $\varepsilon^* = (S_h^*, P_h^*, I_c^*, I_y^*, R_h^*, S_m^*, I_m^*)$ *of the malaria model is locally asymptotically stable if and only if* $R_0 > 1$.

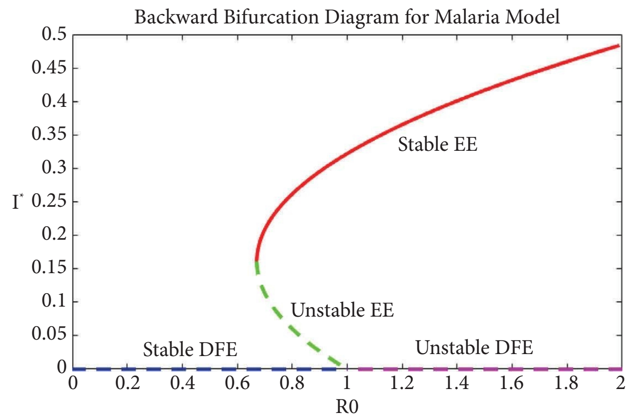


Figure 2: Backward bifurcation diagram for age-structured malaria model.

*Proof.* To show the local stability of the endemic equilibrium point, we use the method of the Jacobian matrix and RH stability criterion. The Jacobian of the malaria model at any point is

$$J(\varepsilon_0) = \begin{pmatrix} D_1 - \lambda & \varphi & 0 & 0 & \beta\Phi & 0 & -V_1 \\ \tau & D_2 - \lambda & 0 & 0 & (1-\Phi)\beta & 0 & 0 \\ 0 & 0 & D_3 - \lambda & 0 & 0 & 0 & V_2 \\ 0 & 0 & \eta & D_4 - \lambda & 0 & 0 & V_3 \\ 0 & 0 & (\omega_1 + \delta_1) & (\omega_2 + \delta_2) & D_5 - \lambda & 0 & 0 \\ 0 & 0 & -V_4 & -V_5 & 0 & D_6 - \lambda & 0 \\ 0 & 0 & V_4 & V_5 & 0 & \lambda_m & D_7 - \lambda. \end{pmatrix}, \tag{57}$$

where $D_1 = -(\tau + \lambda_c + \lambda_y \mu_h)$, $D_2 = -(\varphi + \mu_h)$, $D_3 = -(\mu_{d_1} + \mu_h + \eta + \omega + \delta_1)$, $D_4 = -(\mu_{d_2} + \delta_2 + \omega_2 + \delta_2)$, $D_5 = -(\beta + \mu_h)$, $D_6 = -\mu_m$, $D_7 = -\mu_m$ $V_1 = (K_1 \varepsilon_c S_h^0/N_h^0 + K_1 \varepsilon_y S_h^0/N_h^0)$, $V_2 = K_1 \varepsilon_c S_h^0/N_h^0$, $V_3 = K_1 \varepsilon_y S_h^0/N_h^0$, $V_4 = K_2 \varepsilon_m S_m^0/N_h^0$, $-V_5 = K_2 \varepsilon_m S_m^0/N_h^0$.

By considering the first column and corresponding row of $7 \times 7$ matrix,

$$(D_1 - \lambda)\begin{pmatrix} D_2 - \lambda & 0 & 0 & (1-\Phi)\beta & 0 & 0 \\ 0 & D_3 - \lambda & 0 & 0 & 0 & V_2 \\ 0 & \eta & D_4 - \lambda & 0 & 0 & V_3 \\ 0 & (\omega_1 + \delta_1) & (\omega_2 + \delta_2) & D_5 - \lambda & 0 & 0 \\ 0 & -V_4 & -V_5 & 0 & D_6 - \lambda & 0 \\ 0 & V_4 & V_5 & 0 & \lambda_m & D_7 - \lambda \end{pmatrix}, \tag{58}$$

and if we consider $|J - \lambda I| = 0$, the first column has a diagonal entry. Therefore, one of the eigenvalues is given by $\lambda_1 = D_2 = -(\varphi + \mu_h)$. The reduced matrix becomes

$$(D_1-\lambda)\begin{pmatrix} D_3-\lambda & 0 & 0 & 0 & V_2\\ \eta & D_4-\lambda & 0 & 0 & V_3\\ (\omega_1+\delta_1) & (\omega_2+\delta_2) & D_5-\lambda & 0 & 0\\ -V_4 & -V_5 & 0 & D_6-\lambda & 0\\ V_4 & V_5 & 0 & \lambda_m & D_7-\lambda \end{pmatrix}, \tag{59}$$

and if we consider $|J-\lambda I|=0$, the third column has a diagonal entry. Therefore, the second eigenvalue is $\lambda_2 = D_5 = -(\beta+\mu_h)$.

The reduced matrix becomes

(1) $(D_1-\lambda)\begin{pmatrix} D_3-\lambda & 0 & 0 & V_2\\ \eta & D_4-\lambda & 0 & V_3\\ -V_4 & -V_5 & D_6-\lambda & 0\\ V_4 & V_5 & \lambda_m & D_7-\lambda \end{pmatrix}$.

By considering the second column of 7by7 Jacobian matrix, the reduced matrix after manipulation becomes

(2) $-(\varphi\tau)\begin{pmatrix} D_3-\lambda & 0 & 0 & V_2\\ \eta & D_4-\lambda & 0 & V_3\\ -V_4 & -V_5 & D_6-\lambda & 0\\ V_4 & V_5 & \lambda_m & D_7-\lambda \end{pmatrix}$.

By taking the common of (1) and (2),

(3) $[(D_1-\lambda)-\varphi\tau]\begin{pmatrix} D_3-\lambda & 0 & 0 & V_2\\ \eta & D_4-\lambda & 0 & V_3\\ -V_4 & -V_5 & D_6-\lambda & 0\\ V_4 & V_5 & \lambda_m & D_7-\lambda \end{pmatrix}$.

By considering the fifth column of $7\times 7$ of the Jacobian matrix, the reduced matrix after expanding different columns with corresponding rows becomes

(4) $(\beta\phi\lambda_c)\begin{pmatrix} \eta & D_4-\lambda & 0 & V_3\\ (\omega_1+\delta_1) & (\omega_2+\delta_2) & 0 & 0\\ -V_4 & -V_5 & D_6-\lambda & 0\\ V_4 & V_5 & \lambda_m & D_7-\lambda \end{pmatrix}$.

And by considering the seventh column, the corresponding row of the reduced matrix is

(5) $-(V_1\lambda_c)\begin{pmatrix} \eta & D_4-\lambda & 0\\ -V_4 & -V_5 & D_6-\lambda\\ V_4 & V_5 & \lambda_m \end{pmatrix}$.

By considering (3), (4), and (5),

$$\begin{aligned}&[(D_1-\lambda)-\varphi\tau](D_3-\lambda)[(D_4-\lambda)(D_6-\lambda)(D_7-\lambda)-V_3V_5\lambda_m-V_5(D_6-\lambda)]\\&-V_2[\eta(-V_5\lambda_m-V_5(D_6-\lambda))]+V_2[(D_4-\lambda)V_4\lambda_m+(D_4-\lambda)(D_6-\lambda)V_4].\end{aligned} \tag{60}$$

After manipulation and rearranging, we obtain the characteristic equation:

$$A_5\lambda^5+A_4\lambda^4+A_3\lambda^3+A_2\lambda^2+A_1\lambda+A_0=0. \tag{61}$$

Using the RH stability criteria, we prove that when $R_0>1$, all roots of the polynomial equations have negative real parts. Thus, the endemic equilibrium point $\varepsilon^*$ is locally asymptotically stable if $R_0>1$. □

*3.8. The Global Stability of the Endemic Equilibrium Point*

**Theorem 8.** *The endemic equilibrium point*

$$\varepsilon^* = \left(S_h^*, P_h^*, I_c^*, I_y^*, R_h^*, S_m^*, I_m^*\right) \tag{62}$$

*of the system is globally asymptotically stable if $R_0>1$.*

*Proof.* Let us define an appropriate Lyapunov function $V(x)$ by applying the approach [28] such that

$$V(x)=\sum_{i=1}^{7}\left(X_i-X_i^*-X_i^*X_i^*\ln\left(\frac{X_i}{X_i^*}\right)\right), \tag{63}$$

where $X_i$ represent the population of the compartment $X_i^*$ and are endemic equilibrium points in $R_+^7$, and thus,

$$\begin{aligned}V(x)=&\left(S_h-S_h^*-S_h^*\ln\left(\frac{S_h}{S_h^*}\right)\right)+\left(P_h-P_h^*-P_h^*\ln\left(\frac{P_h}{P_h^*}\right)\right)+\left(I_c-I_c^*-I_c^*\ln\left(\frac{I_c}{I_c^*}\right)\right)\\&+\left(I_y-I_y^*-I_y^*\ln\left(\frac{I_y}{I_y^*}\right)\right)+\left(R_h-R_h^*-R_h^*\ln\left(\frac{R_h}{R_h^*}\right)\right)\\&+\left(S_m-S_m^*-S_m^*\ln\left(\frac{S_m}{S_m^*}\right)\right)+\left(I_m-I_m^*-I_m^*\ln\left(\frac{I_m}{I_m^*}\right)\right).\end{aligned} \tag{64}$$

By differentiating (64) with respect to $t$ and replacing the derivatives in the equation from their respective expressions in the equation of the system, we obtain

$$\begin{aligned}
\frac{dV}{dt} &= (1-\gamma)\Lambda_h + \varphi P_h + \beta\Phi R_h - \left(\tau + \lambda_c + \lambda_y + \mu_h\right)S_h \\
&- \frac{S_h}{S_h^*}\left((1-\gamma)\Lambda_h + \varphi P_h + \beta\Phi R_h - \left(\tau + \lambda_c + \lambda_y + \mu_h\right)S_h\right) \\
&+ \gamma\Lambda_h + \tau S_h + (1-\Phi)\beta R_h - (\varphi + \mu_h)P_h \\
&- \frac{P_h}{P_h^*}\left(\gamma\Lambda_h + \tau S_h + (1-\Phi)\beta R_h - (\varphi + \mu_h)P_h\right) \\
&+ \lambda_C S_h - \left(\mu_{d_1} + \mu_h + \eta + (\omega_1 + \delta_1)\right)I_C \\
&- \frac{I_c}{I_c^*}\left(\lambda_C S_h - \left(\mu_{d_1} + \mu_h + \eta + (\omega_1 + \delta_1)\right)I_C\right) \\
&+ \lambda_y S_h + \eta I_C - \left(\mu_{d_2} + \mu_h + (\omega_2 + \delta_2)\right)I_y \\
&- \frac{I_y}{I_y^*}\left(\lambda_y S_h + \eta I_C - \left(\mu_{d_2} + \mu_h + (\omega_2 + \delta_2)\right)I_y\right) \\
&+ (\omega_2 + \delta_2)I_y + (\omega_1 + \delta_1)I_C - (\beta\phi + (1-\phi)\beta + \mu_h)R_h \\
&- \frac{R_h}{R_h^*}(\omega_2 + \delta_2)I_y + (\omega_1 + \delta_1)I_C - (\beta\phi + (1-\phi)\beta + \mu_h)R_h \\
&+ \gamma\Lambda_m - (\lambda_m + \mu_m)S_m \\
&- \frac{S_m}{S_m^*}\left(\Lambda_m - (\lambda_m + \mu_m)S_m\right) + \lambda_m S_m - \mu_m I_m \\
&- \frac{I_m}{I_m^*}\left(\lambda_m S_m - \mu_m I_m\right),
\end{aligned} \tag{65}$$

simplify equation (65) by gathering negative and positive terms, and yielding: $dV/dt = G_1 - G_2$, where $G_1$ denotes positive terms and $G_2$ denotes negative terms. Therefore, if $G_1 < G_2$, $dV/dt \leq 0$ and $dV/dt = 0$ if and only if $S_h = S_h^*, P_h = P_h^*, I_c = I_c^*, I_y = I_y^*, R_h = R_h^*, S_m = S_m^*, I_m = I_m^*$, hence $V$ is, therefore, the Lyapunov function on $M$. Based on this, we can observe that the biggest compact invariant singleton set in $M = \left\{S_h(t), P_h(t), I_c(t), I_y(t), R_h\ (t), S_m(t), I_m(t) \in M: dV/dt = 0\right\}$ is $\varepsilon^* = (S_h^*, P_h^*, I_c^*, I_y^*, I_m^*)$. Therefore, by the principle of LaSalle [31], the endemic equilibrium $\varepsilon_0$ is globally asymptotically stable in the invariant region $M$ if $G_1 < G_2$ for $R_0 > 1$. □

*3.9. Sensitivity Analysis.* The normalized direct sensitivity index of the variable $R_0$ depends on a parameter $(P_r)$ defined as

$$SI_{P_r}^{R_0} = \frac{\partial R_0}{\partial P_r} \times \frac{P_r}{R_0}. \tag{66}$$

These small shear sensitivities allow us to determine the relative importance of different parameters on malaria transmission and prevalence. The most sensitive parameter in Table 3 has a sensitivity index greater than all other parameters.

Table 3: Sensitivity analysis.

| No. | Sensitivity indices at different parameters | Sign | Sensitivity indices at parameter value |
|---|---|---|---|
| 1 | $S_{\varphi}^{R_0}$ | + | $4.3 \times 10^{-4}$ |
| 2 | $S_{\Lambda_m}^{R_0}$ | + | 1/2 |
| 3 | $S_{K_1}^{R_0}$ | + | 1/2 |
| 4 | $S_{K_2}^{R_0}$ | + | 1/2 |
| 5 | $S_{\varepsilon_y}^{R_0}$ | + | 1 |
| 6 | $S_{\varepsilon_c}^{R_0}$ | + | 1 |
| 7 | $S_{\tau}^{R_0}$ | + | −10.5 |
| 8 | $S_{\mu_h}^{R_0}$ | + | $-1.83 \times 10^{-13}$ |
| 9 | $S_{\mu_m}^{R_0}$ | + | −1 |
| 10 | $S_{\Lambda_h}^{R_0}$ | + | −1/2 |
| 11 | $S_{\gamma}^{R_0}$ | + | −2 |
| 12 | $S_{\omega_2}^{R_0}$ | + | −0.46 |
| 13 | $S_{\delta_2}^{R_0}$ | + | −0.11 |
| 14 | $S_{\mu_{d_1}}^{R_0}$ | + | −0.0006 |
| 15 | $S_{\omega_1}^{R_0}$ | + | −0.047 |
| 16 | $S_{\eta}^{R_0}$ | + | −0.0022 |
| 17 | $S_{\delta_1}^{R_0}$ | + | −0.044 |
| 18 | $S_{\phi}^{R_0}$ | + | −0.78 |

## 4. Numerical Simulation of Integer-Order Malaria Model

The numerical simulations examine the effect of combinations of parameters of the modified model on the transmission of the disease by using MATLAB. The simulation is carried out by taking different values of parameters. The set of parameter values is given in Table 4 whose sources are mainly from literature as well as assumptions. We used differential equation solver ODE (45). The simulations and analysis made are based on these parameter values and initial conditions below.

The following initial conditions have been considered: $S_h(0) = 25891$, $P_h(0) = 8285$, $I_c(0) = 1542$, $I_y(0) = 1350$, $R_h(0) = 1543$, $S_m(0) = 11998$, $I_m(0) = 2601$.

*4.1. Numerical Simulation with Sensitive Parameter.* We consider two sensitive parameters, namely, number of bites on preschool-age human per female mosquito per time and the number of bites on young-age human per female mosquito per time.

## 5. The Fractional Malaria Model and Analysis

There are a certain number of limitations of the models developed via classical differential equations, such as the absence of memory effects and being not able to capture the crossover behavior of a physical or a biological process. "The fractional operator, specifically the ABC operator, comprises

Table 4: Parameter values.

| Parameter | Value | Source |
|---|---|---|
| $\omega_1$ | 0.6415 | Assumption |
| $\delta_1$ | 0.0014 | [15] |
| $\omega_2$ | 0.415 | Assumption |
| $\delta_2$ | 0.00000035 | [15] |
| $\varphi$ | 0.652 | Assumption |
| $\tau$ | 0.9988 | Assumption |
| $\Lambda_h$ | 178 | Assumption |
| $\beta$ | 0.222 | Assumption |
| $\phi$ | 0.00042 | Assumption |
| $\gamma$ | 0.99 | Assumption |
| $\eta$ | 0.997 | Assumption |
| $\mu_{d_1}$ | $2.14 \times 10^{-6}$ | [15] |
| $\mu_{d_2}$ | $9.78 \times 10^{-8}$ | [15] |
| $\mu_m$ | 0.042 | [15] |
| $\mu_h$ | 0.00004 | [15] |
| $\varepsilon_c$ | 0.429 | [15] |
| $\varepsilon_y$ | 0.695 | Assumption |
| $K_1$ | 0.456 | Assumption |
| $K_2$ | 0.574 | Assumption |

the memory effects and the crossover behavior of the model." Memory effect means that the future state of the fractional operator of a given function depends on the current state and the historical behavior of the state [32]. Therefore, to explore the malaria dynamics more realistically, "Some basics of fractional calculus" are reformulated with the replacement of classical derivative by the one having fractional order in ABC sense. Thus, the fractional epidemic model for age-structured malaria model with the nonlocal kernel is formulated through the following system.

### 5.1. Some Basic Concepts from Fractional Calculus

*Definition 9.* Let $f\colon [a,b] \longrightarrow R, a<b$, be abounded and continuous function and let $\alpha \in [0,1]$. The Atangana–Baleanu fractional derivative for a given function of order $\alpha$ in Caputo sense is defined by ${}_a^{\mathrm{ABC}}\mathbb{D}_t^{\alpha} f\ (t) = M(\alpha) / (1-\alpha) \int_a^t df(\tau)/d\tau\, E_\alpha(-\alpha(t-\tau)^\alpha/1-\alpha)d\tau$ where $M(\alpha) = (1\ -\alpha) + \alpha/\Gamma(\alpha)$ denotes $M(0) = M(1) = 1$ and $E_\alpha$ is Mittag-Leffler function, defined by $E_\alpha(z) = \Sigma_{k=0}^{\infty} z^k/\Gamma(\alpha k + 1), \alpha \epsilon C, R_e(\alpha) > 0$.

*Definition 10* (see [33]). Let $f\colon [a,b] \longrightarrow R$ be bounded and continuous function; then, the corresponding fractional integral concerning $AB$ fractional-order derivatives is defined as ${}_a^{ABC}\mathbb{I}_t^{\alpha} f(t) = 1-\alpha/M(\alpha) f(t) + \alpha/M(\alpha)\Gamma(\alpha)\ \int_{t_0}^{t} f(\tau)(t-\tau)^{\alpha-1}d\tau$.

**Theorem 11.** *Let $f\colon [a,b] \Longrightarrow R$ be bounded and continuous function; then, the following result holds as in [32]:*

$$\left\| {}_a^{\mathrm{ABC}}\mathbb{D}_t^{\alpha} f(t) \le \frac{M(\alpha)}{(1-\alpha)} f(t) \right\| = \|\max a \le t \le b(f(t))\|. \tag{67}$$

Furthermore, the Atangana–Baleanu derivative fulfills the Lipschitz condition [32] for two functions $f_1, f_2 \in L(a,b), b>a$; then, the $AB$ fractional derivative satisfies the following inequality:

$$\left\| {}_a^{\mathrm{ABC}}\mathbb{D}_t^{\alpha} f_1(t) \le {}_a^{\mathrm{ABC}}\mathbb{D}_t^{\alpha} f_2(t) \right\| \le L \left\| f_1(t) - f_2(t) \right\|, \tag{68}$$

where $0 < \alpha \le 1$ is the order of fractional derivatives.

The fractional-order system of the differential equation of malaria is proposed as follows:

$$\begin{aligned}
{}_0^{\mathrm{ABC}}\mathbb{D}_t^{\alpha} S_h(t) &= (1-\gamma)\Lambda_h + \varphi P_h + \beta\Phi R_h - \left(\tau + \lambda_c + \lambda_y + \mu_h\right)S_h,\\
{}_0^{\mathrm{ABC}}\mathbb{D}_t^{\alpha} P_h(t) &= \gamma\Lambda_h + \tau S_h + (1-\Phi)\beta R_h - (\varphi + \mu_h)P_h,\\
{}_0^{\mathrm{ABC}}\mathbb{D}_t^{\alpha} I_c(t) &= \lambda_c S_h - \left(\mu_{d_1} + \mu_h + \eta + \omega_1 + \delta_1\right)I_c,\\
{}_0^{\mathrm{ABC}}\mathbb{D}_t^{\alpha} I_y(t) &= \lambda_y S_h + \eta I_c - \left(\mu_{d_2} + \mu_h + \omega_2 + \delta_2\right)I_y,\\
{}_0^{\mathrm{ABC}}\mathbb{D}_t^{\alpha} R_h(t) &= (\omega_2 + \delta_2)I_y + (\omega_1 + \delta_1)I_c - (\beta\Phi + (1-\Phi)\beta + \mu_h)R_h,\\
{}_0^{\mathrm{ABC}}\mathbb{D}_t^{\alpha} S_m(t) &= \Lambda_m - (\lambda_m + \mu_m)S_m,\\
{}_0^{\mathrm{ABC}}\mathbb{D}_t^{\alpha} I_m(t) &= \lambda_m S_m - \mu_m I_m.
\end{aligned} \tag{69}$$

The Atangana–Baleanu ($AB$) derivative is described by the system of DEs, and the mathematical model can be written as

$${}_0^{\mathrm{ABC}}\mathbb{D}_t^{\alpha} X(t) = F_i(t, X(t)), \text{where}, X(t) = \left(S_h(t), P_h(t), I_c(t), I_y(t), R_h(t), S_m(t), I_m(t)\right). \tag{70}$$

In the fractional order of dynamical system (70), $F_i(t, X(t))$ for $i = 1, 2, 3, 4, 5, 6, 7$ are kernels of the dynamical system with initial conditions $S_h(0) = S_0, P_h(0) = P_0, I_c(0) = I_0, I_y(0) = I_0, R_h(0) = R_0, S_m(0) = S_0, I_m(0) = I_0$.

*5.2. Existence and Uniqueness of Solutions.* To show the existence of solution of the given model, we use the Banach fixed point theorem, and to show the existence and uniqueness of the solution, we apply *AB* fractional integral to the proposed model [34]. Let

$$B = E(J) \times E(J) \times E(J) \times E(J) \times E(J) \times E(J) \times E(J) \times E(J) = C[0, T] \tag{71}$$

be the Banach space of real-valued continuous functions defined on an interval $E(J) = [0, T]$ with the corresponding norm defined by

$$\begin{aligned} &\left\| S_h(t), P_h(t), I_c(t), S_y(t), R_h(t), S_m(t), I_m(t) \right\| \\ &= \left\| S_h(t) \right\| + \left\| P_h(t) \right\| + \left\| I_c(t) \right\| + \left\| S_y(t) \right\| + \left\| R_h(t) \right\| + \left\| S_m(t) \right\| + \left\| I_m(t) \right\|, \end{aligned} \tag{72}$$

and the associated sup norm [35].

**Theorem 12** (see [33, 34]). (Lipschitz condition and contraction).

*For each kernel in the fractional model above, there exists a Lipschitz constant $L_i > 0, i = 1, 2, 3, 4, 5, 6, 7$, such that*

$$\left\| F_i(t, X(t)) - F_i(t, X_i(t)) \right\| \leq L_i \left\| X(t) - X_i(t) \right\| \tag{73}$$

*is contraction for $0 \leq L_i < 1$.*

*Proof.* Let the kernel of the first compartment, $F_1$, satisfy the Lipschitz condition and contraction if the inequality given below holds:

$$\begin{aligned} &0 \leq \tau + \mu_h + \frac{K_1\varepsilon_c}{M(N_h)} + \frac{K_1\varepsilon_y}{M(N_h)} < 1, \\ &\left\| F_1(t, S_h) - F_1(t, S_{h_1}) \right\| = \left\| (1-\gamma)\Lambda_h + \varphi P_h + \beta\phi R_h - \left( \tau + \mu_h \left( \frac{K_1\varepsilon_c}{M(N_h)} + \frac{K_1\varepsilon_y}{M(N_h)} \right) I_m \right) S_h \right\| \\ &+ \left\| (1-\gamma)\Lambda_h + \varphi P_h + \beta\phi R_h - \left( \tau + \mu_h \left( \frac{K_1\varepsilon_c}{M(N_h)} + \frac{K_1\varepsilon_y}{M(N_h)} \right) I_m \right) S_h \right\| \\ &+ \leq \left\| \left( \tau + \mu_h \left( \frac{K_1\varepsilon_c}{M(N_h)} + \frac{K_1\varepsilon_y}{M(N_h)} \right) I_m \right) \left( S_h - S_{h_1} \right) \right\| \\ &\leq \left( \tau + \mu_h + \left( \frac{K_1\varepsilon_c}{M(N_h)} + \frac{K_1\varepsilon_y}{M(N_h)} \right) I_m \right) \left\| S_h - S_{h_1} \right\|. \end{aligned} \tag{74}$$

Suppose that

$$L_1 = \left( \tau + \mu_h + \left( \frac{K_1\varepsilon_c}{M(N_h)} + \frac{K_1\varepsilon_y}{M(N_h)} \right) Z_7 \right), \tag{75}$$

where

$$\begin{aligned} &\left\| S_h \right\| = \sup_{t\in J} \left\| S_h(t) \right\| = Z_1, \left\| P_h \right\| = \sup_{t\in J} \left\| P_h(t) \right\| = Z_2, \\ &\left\| I_c \right\| = \sup_{t\in J} \left\| I_c(t) \right\| = Z_3, \\ &\left\| I_y \right\| = \sup_{t\in J} \left\| I_y(t) \right\| = Z_4, \left\| R_h \right\| = \sup_{t\in J} \left\| R_h(t) \right\| = Z_5, \\ &\left\| S_m \right\| = \sup_{t\in J} \left\| S_m(t) \right\| = Z_6, \left\| I_m \right\| = \sup_{t\in J} \left\| I_m(t) \right\| = Z_7 \quad \text{where} \quad \left\| I_m \right\| \leq Z_7 \end{aligned} \tag{76}$$

is bounded function, so

$$\left\|F_1(t,S_h)-F_1\left(t,S_{h_1}\right)\right\|\le L_1\left\|S_h(t)-S_{h_1(t)}\right\|, \tag{77}$$

and thus for $F_1$, the Lipschitz condition is obtained, and if

$$0\le\left(\tau+\mu_h+\frac{K_1\varepsilon_c}{M(N_h)}+\frac{K_1\varepsilon_y}{M(N_h)}\right)Z_7<1, \tag{78}$$

then $F_1$ is contraction. Similarly,

$$\begin{aligned}
L_2 &= (\varphi+\mu_h),\\
L_3 &= \left(\mu_{d_1}+\mu_h+\eta\right)+(\omega_1+\delta_1),\\
L_4 &= \left(\mu_{d_2}+\mu_h+\eta\right)+(\omega_2+\delta_2),\\
L_5 &= \beta\phi+(1-\phi)\beta+\mu_h,\\
L_6 &= \frac{K_2\varepsilon_m(Z_3+Z_4)}{M(N_h)}+\mu_h,\\
L_7 &= \mu_m
\end{aligned} \tag{79}$$

are bounded functions; if $0\le L_i<1, i=2,3,4,5,6,7,$ then $F_i, i=2,3,4,5,6,7,$ are contraction.

Consider the following recursive form for any positive integer $n$:

$$X_n(t)=\frac{1-\alpha}{M(\alpha)}F\left(t,X_{(n-1)}\right)+\frac{\alpha}{M(\alpha)\Gamma(\alpha)}\int_{t_0}^{t}F(\tau,X_{n-1}(\tau))(t-\tau)^{\alpha-1}\mathrm{d}\tau, \tag{80}$$

and we express the difference between the successive terms by using recursive formula in (80).

$$\begin{aligned}
A_n(t) &= X_n(t)-X_{n-1}(t)\\
&= \frac{1-\alpha}{M(\alpha)}\left[F_i(t,X_{n-1}(t))-F_i(t,X_{n-2}(t))\right]\\
&\quad\cdot\frac{\alpha}{M(\alpha)\Gamma(\alpha)}\int_{t_0}^{t}F_i(\tau,X_{n-1}(\tau))-F_i(\tau,X_{n-2}(\tau))(t-\tau)^{\alpha-1}\mathrm{d}\tau.
\end{aligned} \tag{81}$$

From (81), the difference between successive terms is expressed as follows:

$$
\begin{aligned}
A_{1n}(t) &= S_{h_n}(t) - S_{h_{n-1}}(t) = \frac{1-\alpha}{M(\alpha)}\left[F_1\left(t, S_{h_{n-1}}(t)\right) - F_1\left(t, S_{h_{n-2}}(t)\right)\right] \\
&\quad \frac{\alpha}{M(\alpha)\Gamma(\alpha)}\int_0^t F_1\left(\tau, S_{h_{n-1}}(\tau)\right) - F_1\left(\tau, S_{h_{n-2}}(\tau)\right)(t-\tau)^{\alpha-1}\mathrm{d}\tau, \\
A_{2n}(t) &= P_{h_n}(t) - P_{h_{n-1}}(t) = \frac{1-\alpha}{M(\alpha)}\left[F_2\left(t, P_{h_{n-1}}(t)\right) - F_2\left(t, P_{h_{n-2}}(t)\right)\right] \\
&\quad \cdot \frac{\alpha}{M(\alpha)\Gamma(\alpha)}\int_0^t F_2\left(\tau, P_{h_{n-1}}(\tau)\right) - F_2\left(\tau, P_{h_{n-2}}(\tau)\right)(t-\tau)^{\alpha-1}\mathrm{d}\tau, \\
A_{3n}(t) &= I_{c_n}(t) - I_{c_{n-1}}(t) = \frac{1-\alpha}{M(\alpha)}\left[F_3\left(t, I_{c_{n-1}}(t)\right) - F_3\left(t, I_{c_{n-2}}(t)\right)\right] \\
&\quad \cdot \frac{\alpha}{M(\alpha)\Gamma(\alpha)}\int_0^t F_3\left(\tau, I_{c_{n-1}}(\tau)\right) - F_3\left(\tau, I_{c_{n-2}}(\tau)\right)(t-\tau)^{\alpha-1}\mathrm{d}\tau, \\
A_{4n}(t) &= I_{y_n}(t) - I_{y_{n-1}}(t) = \frac{1-\alpha}{M(\alpha)}\left[F_4\left(t, I_{y_{n-1}}(t)\right) - F_4\left(t, I_{y_{n-2}}(t)\right)\right] \\
&\quad \cdot \frac{\alpha}{M(\alpha)\Gamma(\alpha)}\int_0^t F_4\left(\tau, I_{y_{n-1}}(\tau)\right) - F_4\left(\tau, I_{y_{n-2}}(\tau)\right)(t-\tau)^{\alpha-1}\mathrm{d}\tau, \\
A_{5n}(t) &= R_{h_n}(t) - R_{h_{n-1}}(t) = \frac{1-\alpha}{M(\alpha)}\left[F_5\left(t, R_{h_{n-1}}(t)\right) - F_5\left(t, R_{h_{n-2}}(t)\right)\right] \\
&\quad \cdot \frac{\alpha}{M(\alpha)\Gamma(\alpha)}\int_0^t F_5\left(\tau, R_{h_{n-1}}(\tau)\right) - F_5\left(\tau, R_{h_{n-2}}(\tau)\right)(t-\tau)^{\alpha-1}\mathrm{d}\tau, \\
A_{6n}(t) &= S_{m_n}(t) - S_{m_{n-1}}(t) = \frac{1-\alpha}{M(\alpha)}\left[F_6\left(t, S_{m_{n-1}}(t)\right) - F_6\left(t, S_{m_{n-2}}(t)\right)\right] \\
&\quad \cdot \frac{1}{\Gamma(\alpha)}\int_0^t F_6\left(\tau, S_{m_{n-1}}(\tau)\right) - F_6\left(\tau, S_{m_{n-2}}(\tau)\right)(t-\tau)^{\alpha-1}\mathrm{d}\tau, \\
A_{7n}(t) &= I_{m_n}(t) - I_{m_{n-1}}(t) = \frac{1-\alpha}{M(\alpha)}\left[F_7\left(t, I_{m_{n-1}}(t)\right) - F_7\left(t, I_{m_{n-2}}(t)\right)\right] \\
&\quad \cdot \frac{1}{\Gamma(\alpha)}\int_0^t F_7\left(\tau, I_{m_{n-1}}(\tau)\right) - F_7\left(\tau, I_{m_{n-2}}(\tau)\right)(t-\tau)^{\alpha-1}\mathrm{d}\tau,
\end{aligned}
\tag{82}
$$

with initial conditions

$$
\begin{aligned}
&S_{h_0}(t) = S_h(0), P_{h_0}(t) = P_h(0), I_{c_0}(t) = I_c(0), I_{y_0}(t) = I_y(0), \\
&R_{h_0}(t) = R_h(0), S_{m_0}(t) = S_m(0), I_{m_0}(t) = I_m(0).
\end{aligned}
\tag{83}
$$

Equation (70) can be reduced using definition of the norm.

$$
\begin{aligned}
\left\|A_{1n}(t)\right\| &= \left\|S_{h_n}(t) - S_{h_{n-1}}(t)\right\| = \frac{1-\alpha}{M(\alpha)}\left\|F_1\left(t, S_{h_{n-1}}(t)\right) - F_1\left(t, S_{h_{n-2}}(t)\right)\right\| \\
&\quad + \left\|\frac{\alpha}{M(\alpha)\Gamma(\alpha)}\int_0^t F_1\left(\tau, S_{h_{n-1}}(\tau)\right) - F_1\left(\tau, S_{h_{n-2}}(\tau)\right)(t-\tau)^{\alpha-1}\mathrm{d}\tau\right\|.
\end{aligned}
\tag{84}
$$

Applying triangular inequality,

$$\begin{aligned}\left\|S_{h_n}(t)-S_{h_{n-1}}(t)\right\| \leq & \frac{1-\alpha}{M(\alpha)}\left\|F_1\left(t,S_{h_{n-1}}(t)\right)-F_1\left(t,S_{h_{n-2}}(t)\right)\right\| \\ & +\left\|\frac{\alpha}{M(\alpha)\Gamma(\alpha)}\int_0^t F_1\left(\tau,S_{h_{n-1}}(\tau)\right)-F_1\left(\tau,S_{h_{n-2}}(\tau)\right)(t-\tau)^{\alpha-1}d\tau\right\|,\end{aligned} \tag{85}$$

and by integrating (73), we obtained

$$\begin{aligned}\left\|A_{1n}(t)\right\| = \left\|S_{h_n}(t)-S_{h_{n-1}}(t)\right\| \leq & \frac{1-\alpha}{M(\alpha)}L_1\left\|S_{h_n}(t)-S_{h_{n-1}}(t)\right\| \\ & +\frac{t^\alpha}{M(\alpha)\Gamma(\alpha)}L_1\left\|S_{h_n}(t)-S_{h_{n-1}}(t)\right\|\left\|A_{1n}(t)\right\| \\ \leq & \left\|A_{1n-1}(t)\right\|\left(\frac{1-\alpha}{M(\alpha)}+\frac{t^\alpha}{M(\alpha)\Gamma(\alpha)}\right).\end{aligned} \tag{86}$$

Similarly,

$$\begin{aligned}\left\|A_{2n}(t)\right\| &\leq \left\|A_{2n-1}(t)\right\|\left(\frac{1-\alpha}{M(\alpha)}+\frac{t^\alpha}{M(\alpha)\Gamma(\alpha)}\right),\\ \left\|A_{3n}(t)\right\| &\leq \left\|A_{3n-1}(t)\right\|\left(\frac{1-\alpha}{M(\alpha)}+\frac{t^\alpha}{M(\alpha)\Gamma(\alpha)}\right),\\ \left\|A_{4n}(t)\right\| &\leq \left\|A_{4n-1}(t)\right\|\left(\frac{1-\alpha}{M(\alpha)}+\frac{t^\alpha}{M(\alpha)\Gamma(\alpha)}\right),\\ \left\|A_{5n}(t)\right\| &\leq \left\|A_{5n-1}(t)\right\|\left(\frac{1-\alpha}{M(\alpha)}+\frac{t^\alpha}{M(\alpha)\Gamma(\alpha)}\right),\\ \left\|A_{6n}(t)\right\| &\leq \left\|A_{6n-1}(t)\right\|\left(\frac{1-\alpha}{M(\alpha)}+\frac{t^\alpha}{M(\alpha)\Gamma(\alpha)}\right),\\ \left\|A_{7n}(t)\right\| &\leq \left\|A_{7n-1}(t)\right\|\left(\frac{1-\alpha}{M(\alpha)}+\frac{t^\alpha}{M(\alpha)\Gamma(\alpha)}\right).\end{aligned} \tag{87}$$

□

**Theorem 13.** *The mathematical model involving Atangana–Baleanu fractional model given in (69) has solution if there exists $y_0$ such that*

$$\left(\frac{1-\alpha}{M(\alpha)}+\frac{t^\alpha}{M(\alpha)\Gamma(\alpha)}\right)L_i<1, \quad i=1,2,3,4,5,6,7. \tag{88}$$

*Proof.* Using techniques of recursive formula, we obtain

$$\left\|A_{1n}(t)\right\| \leq \left\|S_{h_n}(0)\right\|L_1\left(\frac{1-\alpha}{M(\alpha)}+\frac{t^\alpha}{M(\alpha)\Gamma(\alpha)}\right)^n. \tag{89}$$

Similarly,

$$\begin{aligned}\left\|A_{1n}(t)\right\| &\leq \left\|S_{h_n}(0)\right\|L_1\left(\frac{1-\alpha}{M(\alpha)}+\frac{t^\alpha}{M(\alpha)\Gamma(\alpha)}\right)^n,\\ \left\|A_{2n}(t)\right\| &\leq \left\|P_{h_n}(0)\right\|L_2\left(\frac{1-\alpha}{M(\alpha)}+\frac{t^\alpha}{M(\alpha)\Gamma(\alpha)}\right)^n,\\ \left\|A_{3n}(t)\right\| &\leq \left\|I_{c_n}(0)\right\|L_3\left(\frac{1-\alpha}{M(\alpha)}+\frac{t^\alpha}{M(\alpha)\Gamma(\alpha)}\right)^n,\\ \left\|A_{4n}(t)\right\| &\leq \left\|I_{y_n}(0)\right\|L_4\left(\frac{1-\alpha}{M(\alpha)}+\frac{t^\alpha}{M(\alpha)\Gamma(\alpha)}\right)^n,\\ \left\|A_{5n}(t)\right\| &\leq \left\|R_{h_n}(0)\right\|L_5\left(\frac{1-\alpha}{M(\alpha)}+\frac{t^\alpha}{M(\alpha)\Gamma(\alpha)}\right)^n,\\ \left\|A_{6n}(t)\right\| &\leq \left\|S_{m_n}(0)\right\|L_6\left(\frac{1-\alpha}{M(\alpha)}+\frac{t^\alpha}{M(\alpha)\Gamma(\alpha)}\right)^n,\\ \left\|A_{7n}(t)\right\| &\leq \left\|S_{h_n}(0)\right\|L_7\left(\frac{1-\alpha}{M(\alpha)}+\frac{t^\alpha}{M(\alpha)\Gamma(\alpha)}\right)^n.\end{aligned} \tag{90}$$

Now we are going to show functions which are $S_h, P_h, I_c, I_y, R_h, S_m, I_m$ that are solutions of (69).

Assume

$$S_h(t)-S_h(0)=S_{h_n(t)}-A_{1n}(t), \tag{91}$$

and by repeating the process of recursive formula, we obtain

$$\left\|A_{1n}(t)\right\| \leq \left(\frac{1-\alpha}{M(\alpha)}+\frac{t^\alpha}{M(\alpha)\Gamma(\alpha)}\right)^{n+1}\left(L_1\left\|S_{h_n}(t)-S_{h_{n-1}}(t)\right\|\right)^{n+1}, \tag{92}$$

for $t=y_0$, and (92) becomes

$$\left\|A_{1n}(t)\right\| \leq \left(\frac{1-\alpha}{M(\alpha)} + \frac{y_0^\alpha}{M(\alpha)\Gamma(\alpha)}\right)^{n+1} \left(L_1 \left\|S_{h_n}(t) - S_{h_{n-1}}(t)\right\|\right)^{n+1}, \tag{93}$$

and by taking the limit of (93),

$$n \longrightarrow \infty, \left\|A_{1n}(t)\right\| \longrightarrow \infty, \left(\frac{1-\alpha}{M(\alpha)} + \frac{t^\alpha}{M(\alpha)\Gamma(\alpha)}\right)L_1 < 1. \tag{94}$$

This completes the proof of existence of the solution of the given model using the Banach fixed point theorem; the same is true for the remaining expressions. □

**Theorem 14.** *The Atangana–Baleanu fractional model has a unique solution if*

$$\left(\frac{1-\alpha}{M(\alpha)} + \frac{t^\alpha}{M(\alpha)\Gamma(\alpha)}\right)L_i < 1. \tag{95}$$

*Let $X^* = (S_{h_1}, P_{h_1}, I_{c_1}, I_{y_1}, R_{h_1}, S_{m_1}, I_{m_1})$ be solutions of the proposed fractional model*

$$\begin{aligned} X(t) - X^*(t) = {} & \frac{1-\alpha}{M(\alpha)} F_i(t, X(t)) - F_i(t, X^*(t)) \\ & + \frac{\alpha}{M(\alpha)\Gamma(\alpha)} \int_{t_0}^{t} F_i(\tau, X(\tau)) - F_i(\tau, X^*(\tau))(t-\tau)^{\alpha-1} \mathrm{d}\tau. \end{aligned} \tag{96}$$

By taking the norm of both sides and after integrating, we obtain

$$\left\|X(t) - X^*(t)\right\| \leq \frac{1-\alpha}{M(\alpha)} L_i \left\|X(t) - X^*(t)\right\| + \frac{\alpha}{M(\alpha)\Gamma(\alpha)} L_i \left\|X(t) - X^*(t)\right\|. \tag{97}$$

We have $\|X(t) - X^*(t)\|$ which is common for both sides since

$$1 - \left(\frac{1-\alpha}{M(\alpha)} + \frac{t^\alpha}{M(\alpha)\Gamma(\alpha)}\right)L_i > 0, \tag{98}$$

and we get $\|X(t) - X^*(t)\| = 0$; then, we have $X(t) = X^*(t)$, and thus (69) has unique solution.

**Theorem 15.** *The epidemiologically feasible region of AB fractional model is given by*

$$M = S_h(t), P_h(t), I_c(t), I_y(t), R_h(t), S_m(t), I_m(t) \epsilon R_+^7, \tag{99}$$

*such that*

$$\begin{aligned} 0 \leq {} & S_h(t) + P_h(t) + I_c(t) + I_y(t) + R_h(t) \\ & + S_m(t) + I_m(t) \leq N_h \leq \frac{\Lambda_h}{\mu_h}. \end{aligned} \tag{100}$$

To show positivity, we have to consider the following lemma.

**Lemma 16** (see [36]) (generalized mean value theorem). *Let $f(x) \in C[a,b]$ and ${}_0^{ABC}\mathbb{D}_t^\alpha f(x) \geq 0 \epsilon C \in [a,b]$ when $0 < \alpha \leq 1$. Then, we have*

$$f(a) = f(a) + \frac{1}{\Gamma(\alpha)} {}_0^{ABC}\mathbb{D}_t^\alpha f(\varepsilon)(x-a)^\alpha, \tag{101}$$

when $0 \leq \varepsilon \leq x, \forall_x \in (a,b]$. From the lemma above, if

$$\begin{aligned} & f(x) \in C[0,b], {}_0^{\mathrm{ABC}}\mathbb{D}_t^\alpha f(x) \epsilon C[a,b], \\ & {}_0^{\mathrm{ABC}}\mathbb{D}_t^\alpha f(x) \geq 0, \quad \forall_x \in [0,b], \end{aligned} \tag{102}$$

when $0 < \alpha \leq 1$ $f(x)$ is nondecreasing, and for

$${}_0^{\mathrm{ABC}}\mathbb{D}_t^\alpha f(x) \leq 0, \quad \forall_x \in [0,b], \tag{103}$$

$f(x)$ is nonincreasing. Let us show that $M$ is positively invariant; using the above lemma, we have

$$\begin{aligned} & {}_0^{\mathrm{ABC}}\mathbb{D}_t^\alpha \mid S_h = 0 = (1-\gamma)\Lambda_h + \varphi P_h + \beta\Phi R_h \geq 0, \\ & {}_0^{\mathrm{ABC}}\mathbb{D}_t^\alpha \mid P_h = 0 = \gamma\Lambda_h + \tau S_h + (1-\Phi)\beta R_h \geq 0, \\ & {}_0^{ABC}\mathbb{D}_t^\alpha \mid I_c = 0 = \lambda_c S_h \geq 0. \end{aligned} \tag{104}$$

Similarly, each of the remaining solutions of the model is nonnegative and remains in $M$. To show that the solution of the system is bounded, we have to obtain the fractional derivatives of total population by summing up all the relations in the system, so

$$\begin{aligned} & {}_0^{\mathrm{ABC}}\mathbb{D}_t^\alpha S_h + {}_0^{\mathrm{ABC}}\mathbb{D}_t^\alpha P_h + {}_0^{\mathrm{ABC}}\mathbb{D}_t^\alpha I_c + {}_0^{\mathrm{ABC}}\mathbb{D}_t^\alpha I_y + {}_0^{\mathrm{ABC}}\mathbb{D}_t^\alpha R_h, \\ & {}_0^{\mathrm{ABC}}\mathbb{D}_t^\alpha N_h \leq \Lambda_h - \mu_h N_h \Longrightarrow {}_0^{ABC}\mathbb{D}_t^\alpha N_h + \mu_h N_h \leq \Lambda_h. \end{aligned} \tag{105}$$

By applying Laplace transform on both sides of the above inequality,

$$L\left({}_{0}^{\mathrm{ABC}}\mathbb{D}_t^{\alpha}N_h + \mu_h N_h\right) \leq L(\Lambda_h),$$
$$L(N_h) \leq \left(1 - \frac{\tau\alpha S^{-\alpha}}{(1-\tau)(1-\alpha)}\right)\Bigg)^{-1}\left[\frac{1-\alpha}{(1-\tau)F(\alpha)}\left(1 + \frac{\alpha S^{-\alpha}}{1-\alpha}\right)\frac{\Lambda_h}{S} + N_0\frac{1}{(1-\tau)S}\right], \tag{106}$$

*where*

$$\tau = \frac{-\mu_{h(1-\alpha)}}{F(\alpha)}, \tag{107}$$

*and by applying the inverse Laplace transform [37], the solution is given by*

$$N_h(t) = \frac{\Lambda_h}{\mu_h} - \frac{\Lambda_h}{\mu_h(1-\tau)}\frac{d}{dt}\int_0^t E_{\alpha}\frac{\tau\alpha}{(1-\tau)(1-\tau)}(t-x)^{\alpha}\mathrm{d}x + \frac{1}{(1-\tau)}\left(E_{\alpha}\frac{\tau\alpha t^{\alpha}}{(1-\tau)(1-\alpha)}\right)N(0), \tag{108}$$

*where $E_{\alpha,\beta}$ refers to Mittag-Leffler function, and it has asymptotic behavior.*

$$E_{\alpha,\beta}(z) \approx \Sigma_{\tau=1}^{\omega}\frac{Z^{-\tau}}{F(\beta-\alpha\tau)},$$
$$N_h(t) \longrightarrow \frac{\Lambda_h}{\mu_h}, \tag{109}$$

*as, $t \longrightarrow \infty$, $N_h(t) \leq \Lambda_h/\mu_h$ as, $t \longrightarrow 0$ hence it is a biologically feasible region that means for $t \geq 0$ we have $0 < N_h(t) \leq (N_h(t))/\mu_h$ this indicates that the total human population is bounded. In the same way, mosquito population is also bounded because $N_m(t) \leq \Lambda_m/\mu_m$ as $t \longrightarrow 0$.*

*5.3. Local Stability of Disease-Free Equilibrium Point of Fractional Model.* As for the case of the model with integer derivative (45), the fractional model (69) admits always DFE,

$$\varepsilon_0\left(S_{h_0}, P_{h_0}, 0, 0, R_{h_0}, S_{m_0}, 0\right), \tag{110}$$

and disease-free equilibrium point of (69) is given in (14). As in the case of ODE model (45), we compute the reproduction number $R_0$ using the next-generation matrix approach [38], and the reproduction number of fractional model (69) is given by

$$R_0 = \sqrt{\left(\frac{K_2\varepsilon_m S_m^0}{bN_h^0}\right)\left(\frac{K_1\varepsilon_y S_h^0}{\mu_m N_h^0}\right) + \left(\frac{K_2\varepsilon_m S_m^0}{aN_h^0} + \frac{\eta K_2\varepsilon_m S_m^0}{abN_h^0}\right)\left(\frac{K_1\varepsilon_c S_h^0}{\mu_m N_h^0}\right)}. \tag{111}$$

**Theorem 17.** *The disease-free equilibrium of (69) is locally asymptotically stable if $R_0 < 1$ and unstable if $R_0 > 1$.*

To show the local stability of disease-free equilibrium of (69), we use $7 \times 7$ Jacobian matrix and RH criterion. As indicated in (11), the disease-free equilibrium ($\varepsilon_0$) of (69) is locally asymptotically stable for $R_0 < 1$ and unstable for $R_0 > 1$.

By using the same Lyapunov type function as in (14) of classical model (45), we prove that DFE of fractional model (69) is globally asymptotically stable in $M$ whenever $R_0 \leq 1$. Thus, the following result is valid.

**Theorem 18.** *For any $\alpha \in (0, 1]$, the disease-free equilibrium point $\varepsilon_0$ of model (69) is globally asymptotically stable in the feasible region $M$ if $R_0 < 1$ [39].*

**Theorem 19.** *The endemic equilibrium point $\varepsilon^* = (S_h^*, P_h^*, I_c^*, I_y^*, R_h^*, S_m^*, I_m^*)$ of the malaria model of (69) is locally asymptotically stable if and only if $R_0 > 1$.*

To show the local stability of the endemic equilibrium point, we used the method of the Jacobian matrix and RH stability criterion.

As indicated in (21), endemic equilibrium point $\varepsilon^*$ is locally asymptotically stable if $R_0 > 1$.

**Theorem 20.** *The endemic equilibrium point $\varepsilon^* = (S_h^*, P_h^*, I_c^*, I_y^*, R_h^*, S_m^*, I_m^*)$ of the system is globally asymptotically stable if $R_0 > 1$.*

As we observe from (26) of this paper, $\varepsilon_0$ is globally asymptotically stable in the invariant region $M$ if $G_1 < G_2$ for $R_0 > 1$.

## 6. Numerical Scheme and Simulation of Fractional-Order Model

The numerical scheme for the solution of fractional-order differential equation is defined by Toufik and Atangana [40]. Consider nonlinear FDEs

$$
{}_{0}^{ABC}\mathbb{D}_{t}^{\alpha}X(t) = F_{i}(t, X(t)), X(0) = X_{0}. \tag{112}
$$

The numerical scheme for (112) is defined as in [34].

$$
\begin{aligned}
X_{n+1} = X_{0} &+ \frac{1-\alpha}{M(\alpha)}(t_{n}, X(t_{n})) \\
&+ \frac{\alpha}{M(\alpha)\Gamma(\alpha)}\sum \frac{h^{\alpha} f(t_{k}, X(t_{k}))}{\Gamma(\alpha+2)}(n+1-k)^{\alpha}(n+2-k+\alpha) - (n-k)^{\alpha}(n+2-k+2\alpha) \\
&- \frac{h^{\alpha} f(t_{k-1}, X(t_{k-1}))}{\Gamma(\alpha+2)}(n+1-k)^{\alpha+1} - (n-k)^{\alpha}(n+1-k+\alpha).
\end{aligned}
\tag{113}
$$

By adopting the procedure in [40], the numerical scheme of each compartment in the fractional model (69) takes

$$
\begin{aligned}
S_{h}(t_{n+1}) = S_{h}(t_{0}) &+ \frac{1-\alpha}{M(\alpha)}F_{1}\big(t, S_{h}(t), P_{h}(t), I_{c}(t), I_{y}(t), R_{h}(t), S_{m}(t), I_{m}(t)\big) \\
&+ \frac{\alpha}{M(\alpha)\Gamma(\alpha)}\sum \frac{h^{\alpha}F_{1}\big(t, S_{h}(t), P_{h}(t), I_{c}(t), I_{y}(t), R_{h}(t), S_{m}(t), I_{m}(t)\big)}{\Gamma(\alpha+2)} \\
&\cdot (n+1-k)^{\alpha}(n+2-k+\alpha) - (n-k)^{\alpha}(n+2-k+2\alpha) \\
&- \frac{h^{\alpha}F_{1}\big(t, S_{h}(t), P_{h}(t), I_{c}(t), I_{y}(t), R_{h}(t), S_{m}(t), I_{m}(t)\big)}{\Gamma(\alpha+2)}(n+1-k)^{\alpha+1} - (n-k)^{\alpha}(n+1-k+\alpha), \\
P_{h}(t_{n+1}) = P_{h}(t_{0}) &+ \frac{1-\alpha}{M(\alpha)}F_{2}\big(t, S_{h}(t), P_{h}(t), I_{c}(t), I_{y}(t), R_{h}(t), S_{m}(t), I_{m}(t)\big) \\
&+ \frac{\alpha}{M(\alpha)\Gamma(\alpha)}\sum \frac{h^{\alpha}F2\big(t, S_{h}(t), P_{h}(t), I_{c}(t), I_{y}(t), R_{h}(t), S_{m}(t), I_{m}(t)\big)}{\Gamma(\alpha+2)} \\
&\cdot (n+1-k)^{\alpha}(n+2-k+\alpha) - (n-k)^{\alpha}(n+2-k+2\alpha) \\
&- \frac{h^{\alpha}F_{2}\big(t, S_{h}(t), P_{h}(t), I_{c}(t), I_{y}(t), R_{h}(t), S_{m}(t), I_{m}(t)\big)}{\Gamma(\alpha+2)}(n+1-k)^{\alpha+1} - (n-k)^{\alpha}(n+1-k+\alpha), \\
I_{c}(t_{n+1}) = I_{c}(t_{0}) &+ \frac{1-\alpha}{M(\alpha)}F_{3}\big(t, S_{h}(t), P_{h}(t), I_{c}(t), I_{y}(t), R_{h}(t), S_{m}(t), I_{m}(t)\big) \\
&+ \frac{\alpha}{M(\alpha)\Gamma(\alpha)}\sum \frac{h^{\alpha}F_{3}\big(t, S_{h}(t), P_{h}(t), I_{c}(t), I_{y}(t), R_{h}(t), S_{m}(t), I_{m}(t)\big)}{\Gamma(\alpha+2)} \\
&\cdot (n+1-k)^{\alpha}(n+2-k+\alpha) - (n-k)^{\alpha}(n+2-k+2\alpha) \\
&- \frac{h^{\alpha}F_{3}\big(t, S_{h}(t), P_{h}(t), I_{c}(t), I_{y}(t), R_{h}(t), S_{m}(t), I_{m}(t)\big)}{\Gamma(\alpha+2)}(n+1-k)^{\alpha+1} - (n-k)^{\alpha}(n+1-k+\alpha), \\
I_{y}(t_{n+1}) = I_{y}(t_{0}) &+ \frac{1-\alpha}{M(\alpha)}F_{4}\big(t, S_{h}(t), P_{h}(t), I_{c}(t), I_{y}(t), R_{h}(t), S_{m}(t), I_{m}(t)\big) \\
&+ \frac{\alpha}{M(\alpha)\Gamma(\alpha)}\sum \frac{h^{\alpha}F_{4}\big(t, S_{h}(t), P_{h}(t), I_{c}(t), I_{y}(t), R_{h}(t), S_{m}(t), I_{m}(t)\big)}{\Gamma(\alpha+2)} \\
&\cdot (n+1-k)^{\alpha}(n+2-k+\alpha) - (n-k)^{\alpha}(n+2-k+2\alpha) \\
&- \frac{h^{\alpha}F_{4}\big(t, S_{h}(t), P_{h}(t), I_{c}(t), I_{y}(t), R_{h}(t), S_{m}(t), I_{m}(t)\big)}{\Gamma(\alpha+2)}(n+1-k)^{\alpha+1} - (n-k)^{\alpha}(n+1-k+\alpha),
\end{aligned}
$$

$$
\begin{aligned}
R_h(t_{n+1}) &= R_h(t_0) + \frac{1-\alpha}{M(\alpha)} F_5\big(t, S_h(t), P_h(t), I_c(t), I_y(t), R_h(t), S_m(t), I_m(t)\big) \\
&\quad + \frac{\alpha}{M(\alpha)\Gamma(\alpha)} \sum \frac{h^\alpha F_5\big(t, S_h(t), P_h(t), I_c(t), I_y(t), R_h(t), S_m(t), I_m(t)\big)}{\Gamma(\alpha+2)} \\
&\quad \cdot (n+1-k)^\alpha (n+2-k+\alpha) - (n-k)^\alpha (n+2-k+2\alpha) \\
&\quad - \frac{h^\alpha F_5\big(t, S_h(t), P_h(t), I_c(t), I_y(t), R_h(t), S_m(t), I_m(t)\big)}{\Gamma(\alpha+2)} (n+1-k)^{\alpha+1} - (n-k)^\alpha (n+1-k+\alpha), \\
S_m(t_{n+1}) &= S_m(t_0) + \frac{1-\alpha}{M(\alpha)} F_6\big(t, S_h(t), P_h(t), I_c(t), I_y(t), R_h(t), S_m(t), I_m(t)\big) \\
&\quad + \frac{\alpha}{M(\alpha)\Gamma(\alpha)} \sum \frac{h^\alpha F_6\big(t, S_h(t), P_h(t), I_c(t), I_y(t), R_h(t), S_m(t), I_m(t)\big)}{\Gamma(\alpha+2)} \\
&\quad \cdot (n+1-k)^\alpha (n+2-k+\alpha) - (n-k)^\alpha (n+2-k+2\alpha) \\
&\quad - \frac{h^\alpha F_6\big(t, S_h(t), P_h(t), I_c(t), I_y(t), R_h(t), S_m(t), I_m(t)\big)}{\Gamma(\alpha+2)} (n+1-k)^{\alpha+1} - (n-k)^\alpha (n+1-k+\alpha), \\
I_m(t_{n+1}) &= I_m(t_0) + \frac{1-\alpha}{M(\alpha)} F_7\big(t, S_h(t), P_h(t), I_c(t), I_y(t), R_h(t), S_m(t), I_m(t)\big) \\
&\quad + \frac{\alpha}{M(\alpha)\Gamma(\alpha)} \sum \frac{h^\alpha F_7\big(t, S_h(t), P_h(t), I_c(t), I_y(t), R_h(t), S_m(t), I_m(t)\big)}{\Gamma(\alpha+2)} \\
&\quad \cdot (n+1-k)^\alpha (n+2-k+\alpha) - (n-k)^\alpha (n+2-k+2\alpha) \\
&\quad - \frac{h^\alpha F_7\big(t, S_h(t), P_h(t), I_c(t), I_y(t), R_h(t), S_m(t), I_m(t)\big)}{\Gamma(\alpha+2)} (n+1-k)^{\alpha+1} - (n-k)^\alpha (n+1-k+\alpha),
\end{aligned}
\tag{114}
$$

for step size $h(t_m, t_{m-1})$.

In the numerical simulation of dynamics of malaria disease, two categories of the species are considered: the host population which contains the human population and the vector which consists of mosquito. The two species are interconnected with each other. The effect of embedded parameter is shown on the dynamics of both species. We used the numerical technique developed by Toufik and Atangana.

## 7. Result and Discussion

The susceptible human population decreases rapidly as shown in Figure 3. This indicates that the susceptible human population will continue to join the infected class; as a result, the infected population will increase due to high biting rate of mosquito and high probability transmission rate from the infected mosquito to the susceptible human. $R_0 = 1.622$ which is greater than one; this indicates that the mosquito vector is continuously increasing. It supports the theorem for stability of endemic equilibrium point that the disease is endemic when $R_0 > 1$.

Figure 4 shows the distribution of population for different classes with time. Thus, the susceptible human population decreases due to the presence of infective mosquito with high biting rate of mosquito for the first few days. Since the infective vector bites the susceptible human, the susceptible human becomes infected and goes to the infected human compartments; then, the susceptible population decreases and the infected human population increases. After some interval of time, they go to zero due to increment of protected class, that is, as protected class increases, susceptible vector and infected vector class decrease due to lack of meal for their egg; then, the disease-free equilibrium point exists and is stable. The existence of this condition is due to the fact that $R_0 = 2.827 \times 10^{-5}$ which is less than one. This supports the theorem that the stability of disease-free equilibrium point exists when $R_0 < 1$, i.e., the society is free from the disease when $R_0 < 1$.

We also evaluated sensitivity indices of the parameter values shown in Table 2. In the case of malaria transmission, the most sensitive parameter is the rate of mosquito bites or the number of bites in people of preschool age $(\varepsilon_c)$ and young age $(\varepsilon_y)$; other parameters include the probability of transmission from an infectious mosquito to a susceptible person or a portion of the bite that successfully infects human $(K_1)$ and the probability of disease transmission from infectious human to susceptible vector or a portion of the bite that successfully infects mosquito. As shown in Figure 4, the number of bites of mosquito increases and the susceptible human population decreases because when the contact between mosquito and the

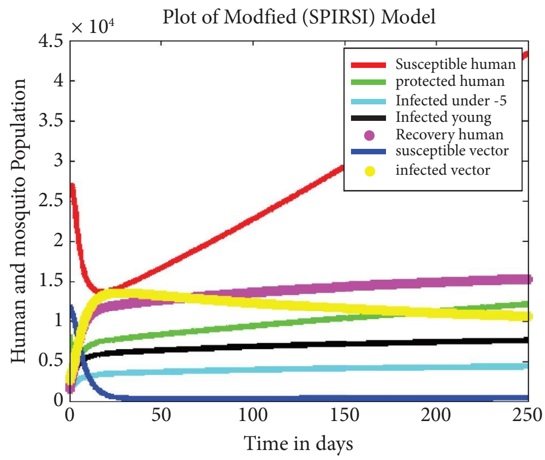


Figure 3: Human mosquito plot shows that susceptible human populations decrease rapidly. This indicates that the susceptible human population will continue to join the infected class $R_0 = 1.622$.

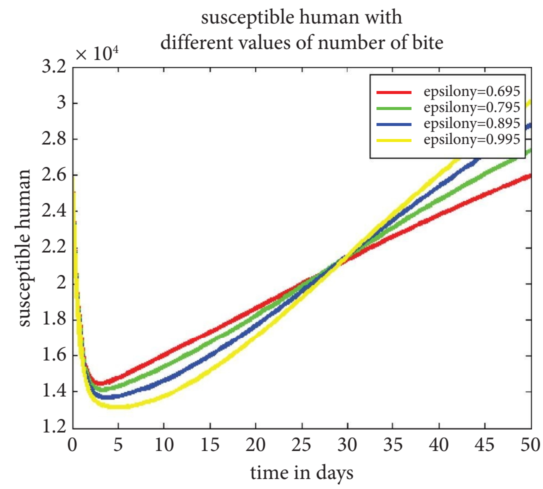


Figure 5: As the number of bites of mosquito increases, the susceptible human population decreases.

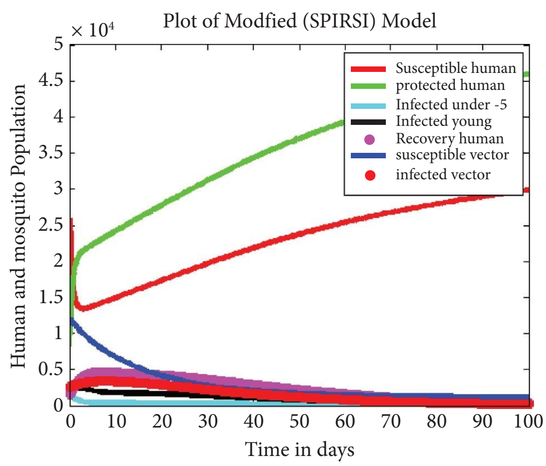


Figure 4: Human mosquito for DFE plot which shows susceptible human population decreases due to the presence of infective mosquito with high biting rate for the first few days.

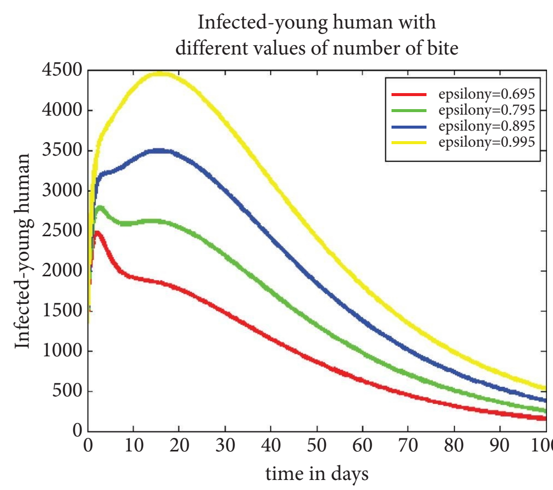


Figure 6: The number of infected young humans increases as the number of bites increases.

two human age levels increases, the force of infection increases and individuals go to the infected class to increase the infected human class as shown in Figure 5. As the number of bites increases, the population of susceptible vector decreases because of increase in infected vector for some time interval initially and then decreases because infected vector goes to the susceptible human class to increase force of infection as shown in Figures 6–8. Susceptible human population decreases in three directions: firstly because of natural death rate, secondly because of increment in force of infection as shown in Figure 4, and thirdly because of increment in transfer rate tau ($\tau$) of human from susceptible class to protected class as shown in Figures 9 and 10 to increase protected class individuals as shown in Figure 11. As explained in assumption part, protection class is the class with individuals who use intervention mechanisms like ITNs and IRS; if individuals who use such control mechanisms increase, the force of infection decreases because of decrease in mosquito vector with lack of meal for their egg production. As shown in Figures 3 and 12, the number of infected humans decreases as the number of recovered humans increases because of increment in natural recovery rate and treatment rate, so this increment in recovery rate is one way to increase protected class individuals; increment in protected class is our target to control malaria disease; because of increment in protection class and recovery rate, infected preschool-age and young-age human population decreases as shown in Figures 13–15.

In Figures 16 and 17, we show the global asymptotic stability of the proposed model by varying the initial conditions of each compartment for time being, and to save time and space, we show only two compartments, namely, susceptible humans and infected preschool humans.

As indicated in Figures 18 and 19, as fractional order $\alpha$ approaches 1 or integer order, the susceptible human population decreases which is similar to that of classical model result, that is, as the biting rate of mosquito increases, the susceptible human population decreases. The majority of

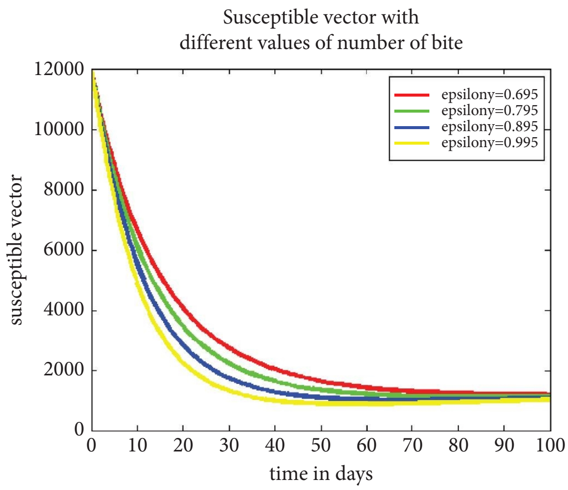


Figure 7: As the number of bites increases, the population of susceptible vector decreases because of the increment of infected vector.

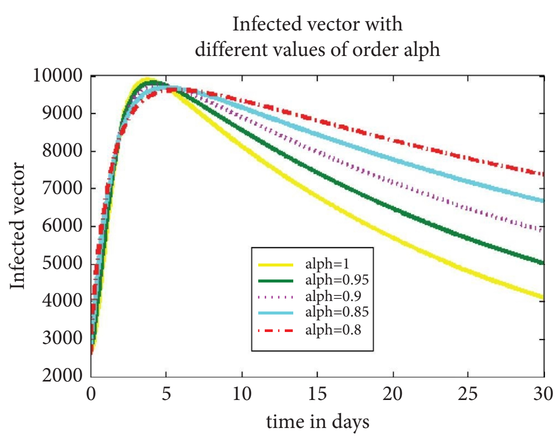


Figure 8: The result shows that the infected vector population is increased for initial time interval then after decrease as time increase.

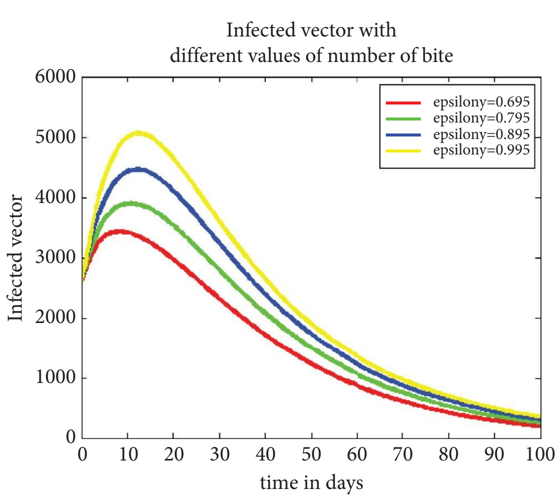


Figure 9: The population of infected vector increases for initial time interval and then decreases.

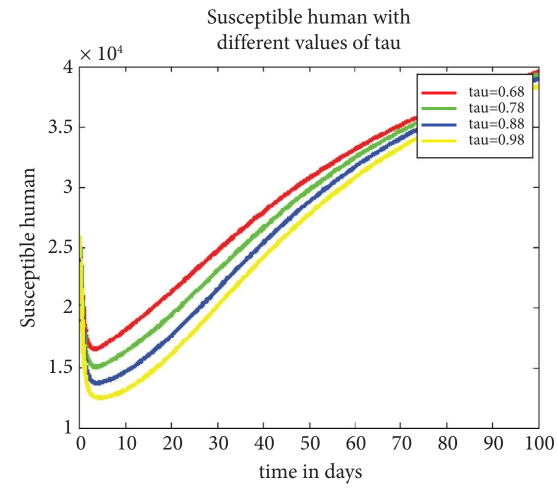


Figure 10: Susceptible population decreases as increases transfer rate ($\tau$) of human from susceptible to protected class.

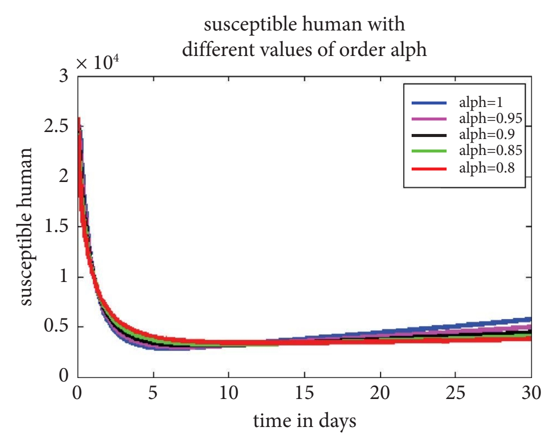


Figure 11: The dynamics of susceptible population with fractional order $\alpha$ which show the decay behavior for the given time $t$.

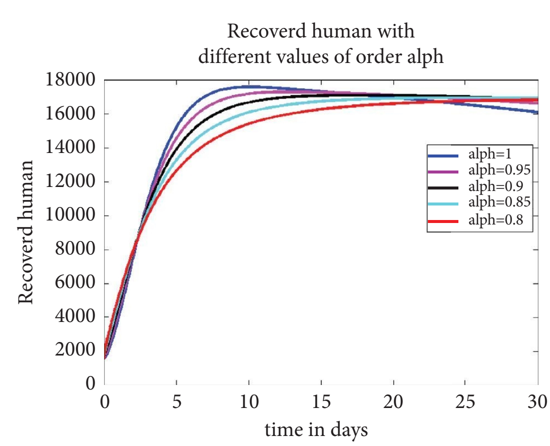


Figure 12: The result of recovered human population with fractional order Îś shows that the recovery is increased for some time interval.

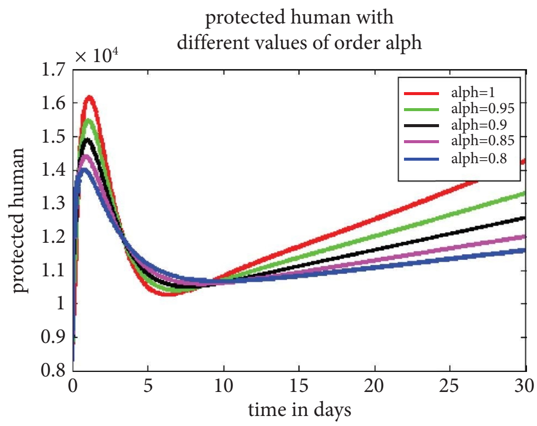


Figure 13: The dynamics of protected human with fractional order $\alpha$ which show protected individuals increased for initial time interval and decreasing behavior for some time; and then increase finally.

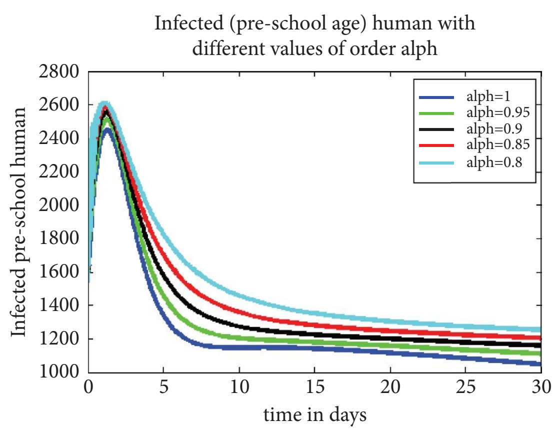


Figure 14: The result shows that the infected preschool-age human increased for the initial interval of time and then strictly slow or decrease as time increase.

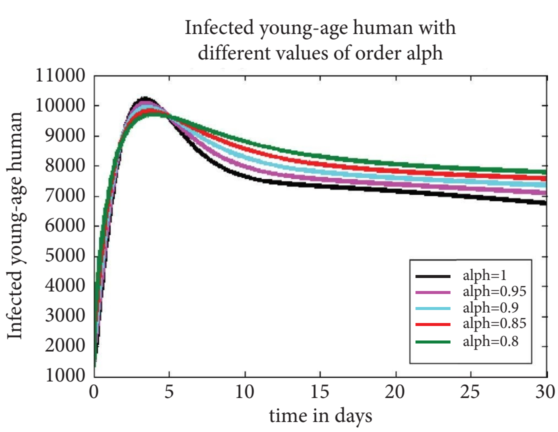


Figure 15: As the result showed that the infected young human increased for the initial interval of time and then decreased as that of infected preschool-age human, but the decrement is not strict.

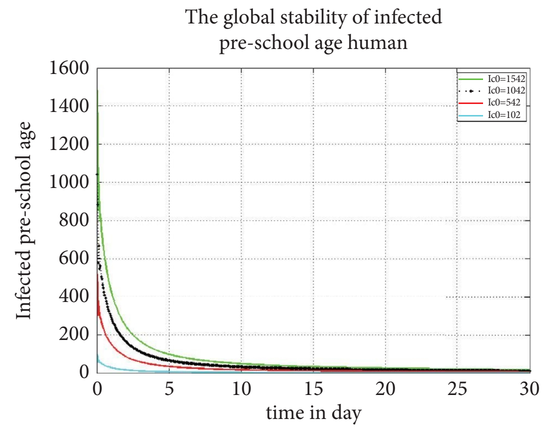


Figure 16: Global stability of infected preschool humans.

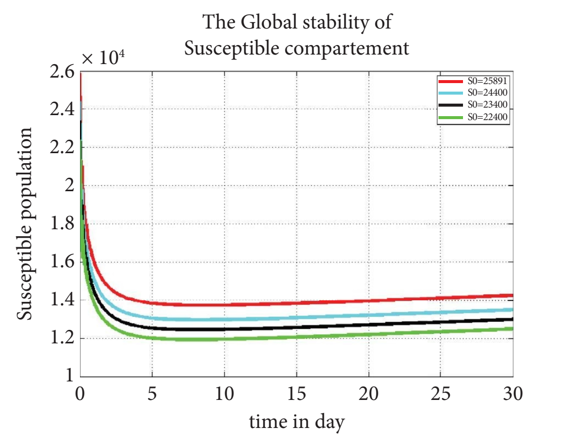


Figure 17: Global stability of susceptible human compartment.

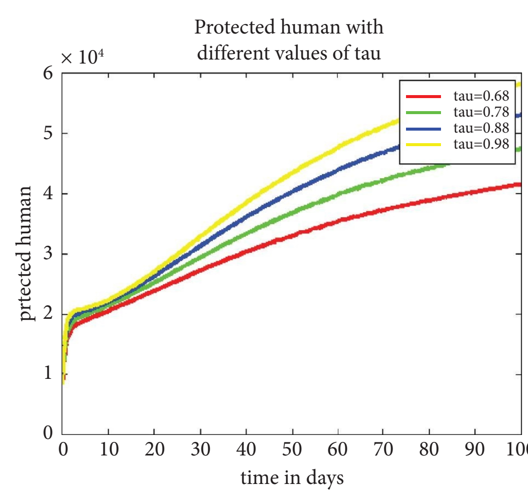


Figure 18: As the value of $\tau$ increases, the protected class also increases.

fractional-order model simulation results are roughly similar to those of classical order model simulation results when fractional order $\alpha \longrightarrow 1$. However, as many studies have shown, the model with fractional derivatives (Atangana–Baleanu in Caputo sense) is superior to the model with integer-order derivatives. Based on theorem (21), we have demonstrated that even in the disease-free equilibrium, there is a chance of an

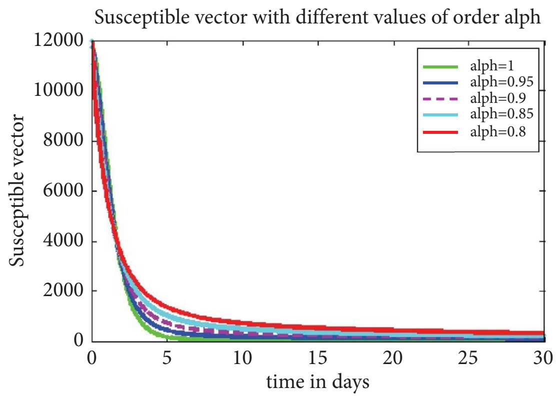


Figure 19: The result of susceptible vector population with fractional order alpha shows that the susceptible vector population decreases because of infection in vector population.

endemic equilibrium when $R_0 < 1$ experiences backward bifurcation; this suggests that society may not fully comprehend the extent of malaria prevalence in the population. When the level of malaria endemicity expressed only by the size of the basic reproductive number is less than one, the disease can disappear but still persist (at very high endemic levels).

## 8. Conclusion

Integer- and fractional-order models were presented for the dynamics of malaria in human hosts with varying ages. A system of differential equations model with five human state variables and two mosquito state variables was examined. We demonstrated the existence of an area in which the model is both mathematically and epidemiologically well posed. The equilibrium point devoid of disease was discovered, and its stability was examined. We identified the basic reproduction number $R_0$ in terms of the model parameters that measure the intensity of the transmission of the disease. It has been demonstrated that during the course of the infectious period, $R_0$ predicts the anticipated number of additional infections (in mosquitoes and people) from one infectious individual (human or mosquito). It was also established that for the basic reproduction number $R_0 < 1$, the disease-free equilibrium point emerges. We showed that the endemic equilibrium point is unique for $R_0 > 1$, and also we showed numerical result for both fractional- and integer-order models. For the numerical simulation of integer order, we used ODE (45), and we used numerical technique developed by Toufik and Atangana for fractional order. *Plasmodium* parasites cause malaria. Since malaria is a global problem, the following measures should be taken to eradicate the disease. The biological explanation of (21) is that when backward bifurcation occurs, malaria can still exist in the community even when $R_0 < 1$, and such situation can lead to misunderstandings about malaria eradication programs. Responsible bodies like policy makers may think they have succeeded in bringing $R_0$ under one and hope malaria will disappear. Unfortunately, if backward bifurcation occurs, there will be a large endemic equilibrium due to the hysteresis that occurs when $R_0 < 1$.

(i) Our results in (21) indicate that responsible bodies need to increase the culture of using different control mechanisms like ITNs and IRS including different medical treatments to avoid backward bifurcation or inverse bifurcation.

(ii) Since the model indicates that the probability of disease transmission rate and mosquito biting rate play a major role in the disease's spread, efforts should be made to reduce mosquito populations and biting rates through biological or chemical means, or any other method that will lower the rate of malaria infection.

(iii) Government agencies with accountability should start and continue efficient programs to guarantee that public health decision makers take into account intervention strategies aimed at reducing mosquito populations and biting rates when controlling malaria. Furthermore, we plan to expand the model in subsequent work to encompass

  (a) Effects of different constant control mechanisms on malaria prevalence, optimal control, and cost analysis.
  (b) The effects of temperature and rainfall on the spread of malaria on the mortality and survival probabilities via optimal control.
  (c) Different fractional-order derivatives and integer-order derivatives, comparing their results and performing backward and forward bifurcation to identify the prevalence of malaria disease.

## Data Availability

The data used to support the findings of this study are included within the article. Actually, for the simulation, we used data from other articles. The papers are correctly referenced.

## Conflicts of Interest

The authors declare that they have no conflicts of interest.

## Acknowledgments

The first author would like to thank the second author for his help in methodology and formal analysis.

## References

[1] P. Bedi, A. Khan, A. Kumar, and T. Abdeljawad, "Computational study of fractional-order vector borne diseases model," *Fractals*, vol. 30, no. 5, 2022.

[2] T. Bakary, S. Boureima, and T. Sado, "A mathematical model of malaria transmission in a periodic environment," *Journal of Biological Dynamics*, vol. 12, no. 1, pp. 400–432, 2018.

[3] J. C. Koella, "On the use of mathematical models of malaria transmission," *Acta Tropica*, vol. 49, no. 1, pp. 1–25, 1991.

[4] J. L. Aron and R. M. May, "The population dynamics of malaria," *Population and Community Biology*, pp. 139–179, Springer, Boston, MA, USA, 1982.

[5] Who, *World Malaria Report*, WHO, Geneva, Switzerland, 2018.
[6] Who Global, *World Malaria Report*, WHO, Geneva, Switzerland, 2019.
[7] R. F. Schumacher and E. Spinelli, "Malaria in children," *Mediterranean Journal of Hematology and Infectious Diseases*, vol. 4, no. 1, Article ID e2012073, 2012.
[8] A. Deribew, T. Dejene, B. Kebede et al., "Incidence, prevalence and mortality rates of malaria in Ethiopia from 1990 to 2015: analysis of the global burden of diseases 2015," *Malaria Journal*, vol. 16, no. 1, pp. 271–277, 2017.
[9] T. Girum, T. Shumbej, and M. Shewangizaw, "Burden of malaria in Ethiopia, 2000-2016: findings from the global health estimates 2016," *Tropical Diseases, Travel Medicine and Vaccines*, vol. 5, no. 1, p. 11, 2019.
[10] M. Moshinsky, *A Short History of Mathematical Population Dynamics*, Springer, London, UK, 1959.
[11] G. E. S. Dhillon and C. S. Aggarwal, *Symposium: Tropical Pediatrics II and Control of Malaria*, Springer, London, UK, 1999.
[12] N. White, "Antimalarial drug resistance and combination chemotherapy," *Philosophical Transactions of the Royal Society of London Series B: Biological Sciences*, vol. 354, no. 1384, pp. 739–749, 1999.
[13] M. Zahle and H. Ziezold, "Fractional derivatives of Weierstrass-type functions," *Journal of Computational and Applied Mathematics*, vol. 76, no. 1-2, pp. 265–275, 1996.
[14] A. I. K. Butt, W. Ahmad, M. Rafiq, N. Ahmad, and M. Imran, "Optimally analyzed fractional Coronavirus model with Atangana–Baleanu derivative," *Results in Physics*, vol. 53, Article ID 106929, 2023.
[15] J. Klinck, "Transmission model details," *Philippine Science Letters*, vol. 5, no. 2, pp. 1–3, 2016.
[16] K. A. Abro, "Ananalytic study of bioheat transfer Pennes model via modern non-integers differential techniques," *European Physical Journal A: Hadrons and Nuclei*, vol. 123, 2021.
[17] K. S. Miller and B. Ross, *An Introduction to the Fractional Calculus and Fractional Differential Equations*, John-Wily and Sons. Inc, New York, NY, USA, 1993.
[18] W. Gao, P. Veeresha, H. M. Baskonus, D. G. Prakasha, and P. Kumar, "A new study of unreported cases of 2019-nCOV epidemic outbreaks," *Chaos, Solitons and Fractals*, vol. 138, Article ID 109929, 2020.
[19] Y. OztUrk and M. Unal, "Numerical solution of fractional differential equations using fractional Chebyshev polynomials," *Asian-European Journal of Mathematics*, vol. 15, no. 03, pp. 1100–1115, 2022.
[20] Z. Odibat and D. Baleanu, "Numerical simulation of initial value problems with generalized Caputo-type fractional derivatives," *Applied Numerical Mathematics*, vol. 156, pp. 94–105, 2020.
[21] D. Baleanu, G. C. Wu, and S. Zeng, "Chaos analysis and asymptotic stability of generalized Caputo fractional differential equations," *Chaos, Solitons and Fractals*, vol. 102, pp. 99–105, 2017.
[22] N. Chitnis, J. M. Cushing, and J. M. Hyman, "Bifurcation analysis of a mathematical model for malaria transmission," *SIAM Journal on Applied Mathematics*, vol. 67, no. 1, pp. 24–45, 2006.
[23] N. R. Chitnis, "Using mathematical models in controlling the spread of malaria," *Mathematics*, vol. 11, no. 7, pp. 1–124, 2005.
[24] K. O. Okosun, "Modelling the impact of drug resistance in malaria transmission and its optimal control analysis," *International Journal of the Physical Sciences*, vol. 6, no. 28, pp. 6479–6487, 2011.
[25] G. T. Azu-Tungmah, F. T. Oduro, and G. A. Okyere, "Optimal control analysis of an age-structured malaria model incorporating children under five years and pregnant women," *Journal of Advances in Mathematics and Computer Science*, vol. 30, no. 6, pp. 1–23, 2019.
[26] A. S. Kalula, E. Mureithi, T. Marijani, and I. Mbalawata, "An age-structured model for transmission dynamics of malaria with infected immigrants and asymptomatic carriers," *Tanzania Journal of Science*, vol. 47, no. 3, pp. 953–968, 2021.
[27] S. Gebremichael and T. Mekonnen, "Impact of climatic factors and intervention strategies on the dynamics of malaria in Ethiopia: a mathematical model analysis," *International Journal of Sciences: Basic and Applied Research*, vol. 54, no. 4, pp. 120–150, 2020.
[28] M. Martcheva, *An Introduction to Mathematical Epidemiology*, Springer, New York, NY, USA, 2013.
[29] A. I. K. Butt, W. Ahmad, M. Rafiq, N. Ahmad, and M. Imran, "Computationally efficient optimal control analysis for the mathematical model of Coronavirus pandemic," *Expert Systems with Applications*, vol. 234, Article ID 121094, 2023.
[30] D. Aldila and M. Angelina, "Optimal control problem and backward bifurcation on malaria transmission with vector bias," *Heliyon*, vol. 7, no. 4, Article ID e06824, 2021.
[31] N. Bame, S. Bowong, J. Mbang, G. Sallet, and J. J. Tewa, "Global stability analysis for seis models with n latent classes," *Mathematical Biosciences and Engineering*, vol. 5, no. 1, pp. 20–33, 2008.
[32] A. Omame, M. Abbas, C. Onyenegecha, M. Abbas, and C. P. Onyenegecha, "A fractional-order model for COVID-19 and tuberculosis co-infection using Atangana–Baleanu derivative," *Chaos, Solitons and Fractals*, vol. 153, Article ID 111486, 2021.
[33] D. D. Pawar, W. D. Patil, and D. K. Raut, "Fractional Order Mathematical Model," *Chaos, Solitons and Fractals*, vol. 39, no. 1, pp. 197–214, 2021.
[34] C. T. Deressa and G. F. Duressa, "Analysis of Atangana-Baleanu fractional-order SEAIR epidemic model with optimal control," *Advances in Difference Equations*, vol. 2021, no. 1, p. 174, 2021.
[35] D. Kumar, J. Singh, M. Al Qurashi, and D. Baleanu, "A new fractional SIRS-SI malaria disease model with application of vaccines, antimalarial drugs, and spraying," *Advances in Difference Equations*, vol. 2019, no. 1, p. 278, 2019.
[36] Z. M. Odibat and N. T. Shawagfeh, "Generalized Taylor's formula," *Applied Mathematics and Computation*, vol. 186, no. 1, pp. 286–293, 2007.
[37] D. Baleanu and A. Fernandez, "On some new properties of fractional derivatives with Mittag-Leffler kernel," *Communications in Nonlinear Science and Numerical Simulation*, vol. 59, pp. 444–462, 2018.
[38] O. Diekmann, J. A. P. Heesterbeek, and J. A. J. Metz, "On the definition and the computation of the basic reproduction ratio R0 in models for infectious diseases in heterogeneous populations," *Journal of Mathematical Biology*, vol. 28, no. 4, pp. 365–382, 1990.
[39] I. A. Rus, "Ulam stabilities of ordinary differential equations in a Banach space," *Carpathian Journal of Mathmatics*, vol. 26, no. 1, pp. 103–107, 2010.
[40] M. Toufik and A. Atangana, "New numerical approximation of fractional derivative with non-local and non-singular kernel: application to chaotic models," *European Physical Journal A: Hadrons and Nuclei*, vol. 132, no. 10, pp. 444–516, 2017.